Applied Materials Today 22 (2021) 100939

Contents lists available at ScienceDirect

Applied Materials Today

journal homepage: www.elsevier.com/locate/apmt

Electrochemistry: A basic and powerful tool for micro- and nanomotor fabrication and characterization

Albert Serrà [a,b,c,*], José García-Torres [d,e,*]

[a] Empa, Swiss Federal Laboratories for Materials Science and Technology, Laboratory for Mechanics of Materials and Nanostructures, Feuerwerkerstrasse 39,CH-3602 Thun, Switzerland
[b] Departament de Ciència de Materials i Química Física, Grup d'Electrodeposició de Capes Primes i Nanoestructures (GE-CPN), Universitat de Barcelona, Martí i Franquès, 1, E-08028 Barcelona, Catalonia, Spain
[c] Institute of Nanoscience and Nanotechnology (IN^{2}UB), Universitat de Barcelona, Barcelona, Catalonia, Spain
[d] Biomaterials, Biomechanics and Tissue Engineering, Department of Materials Science and Engineering, EEBE, Universitat Politècnica de Catalunya, c/Eduard Maristany, 10-14, E-08019 Barcelona, Spain
[e] Barcelona Research Center for Multiscale Science and Engineering, Universitat Politècnica de Catalunya, c/Eduard Maristany 10-14, E-08019 Barcelona, Spain

ARTICLE INFO

Article history:
Received 28 October 2020
Revised 31 December 2020
Accepted 6 January 2021

Keywords:
Electrodeposition
Micromotor
Nanomotor
Biomedical applications
Environmental applications

ABSTRACT

Electrochemistry, although an ancient field of knowledge, has become of paramount importance in the synthesis of materials at the nanoscale, with great interest not only for fundamental research but also for practical applications. One of the promising fields in which electrochemistry meets nanoscience and nanotechnology is micro/nanoscale motors. Micro/nano motors, which are devices able to perform complex tasks at the nanoscale, are commonly multifunctional nanostructures of different materials - metals, polymers, oxides- and shapes -spheres, wires, helices- with the ability to be propelled in fluids. Here, we first introduce the topic of micro/nanomotors and make a concise review of the field up to day. We have analyzed the field from different points of view (e.g. materials science and nanotechnology, physics, chemistry, engineering, biology or environmental science) to have a broader view of how the different disciplines have contributed to such exciting and impactful topic. After that, we focus our attention on describing what electrochemical technology is and how it can be successfully used to fabricate and characterize micro/nanostructures composed of different materials and showing complex shapes. Finally, we will review the micro and nanomotors fabricated using electrochemical techniques with applications in biomedicine and environmental remediation, the two main applications investigated so far in this field. Thus, different strategies have thus been shown capable of producing core-shell nanomaterials combining the properties of different materials, multisegmented nanostructures made of, for example, alternating metal and polymer segments to confer them with flexibility or helicoidal systems to favor propulsion. Moreover, further functionalization and interaction with other materials to form hybrid and more complex objects is also shown.

1. Introduction

Can we imagine a world where surgeries or environmental protection actions are performed by micro/nanorobots? Probably not for most of the society but we as a scientist know that it will be real in the coming years. Already in the mid of last century (late 1950s) the inspiring talk "There's Plenty of Room at the Bottom" by Richard Feynman or science fiction movies like *Fantastic Voyage* already envisioned the era of tiny machines. Nowadays, such robots are starting being a reality in our society. Scientist all over the world are developing small-scale structures able to swim in different and complex environments and to perform multiple and arduous tasks like in the inner body giving rise to the exciting field of nano and microrobotics [1–3].

However, propelling objects at the micro/nanoscale is not an easy task as "the rules of the game" at such scales are different: motion at low Reynolds number is dominated by viscous forces and Brownian motion become significant at small length scales

* Corresponding authors at: Empa, Swiss Federal Laboratories for Materials Science and Technology, Laboratory for Mechanics of Materials and Nanostructures, Feuerwerkerstrasse 39,CH-3602 Thun, Switzerland.
E-mail addresses: a.serra@ub.edu (A. Serrà), jose.manuel.garcia-torres@upc.edu (J. García-Torres).

https://doi.org/10.1016/j.apmt.2021.100939

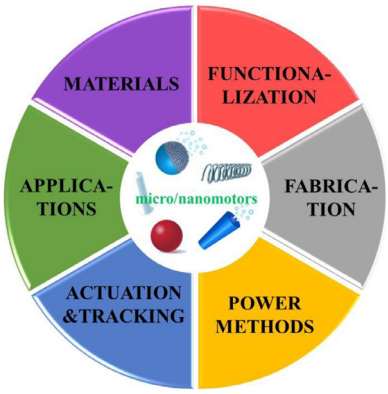

Fig. 1. Representation showing the main disciplines involved in the field of micro/nanomotors.

[4,5]. Thus, designing and fabricating new micro/nanorobots for a myriad of applications are among the most exciting challenges nowadays. To succeed in such challenge, it is necessary to approach it by joining efforts from different disciplines and points of view: (i) materials science & nanotechnology: selection and preparation of new materials using different microfabrication techniques [6,7], (ii) chemistry: chemical synthesis of materials as well as their modification and incorporation of new properties through, for example, surface functionalization or coating [8,9], (iii) physics: experimental control of the propulsion of the nano- and micromotors and theoretical study about the mechanism responsible of the motion [10,11], (iv) engineering: development of the setup for controlling and tracking the motion in real applications (e.g. human body) [12,13] or (v) biological and environmental science: studying the viability of such nanostructures for health and environmental applications [14,15]. As stated above, all those disciplines must be interrelated to properly design, synthesize, modify, actuate and study their applicability in real situations to succeed in the near future as depicted in Fig. 1.

The goal of this review is two-fold: On one hand, to give an introductory overview of the microrobots field in terms of materials, shapes and common techniques for the fabrication and actuation of the structures, understanding the different propulsion mechanisms. And on the other hand, focus our attention on how electrochemistry has been positioned as a powerful tool not only for the fabrication of the microrobots but also for their characterization and how these electrodeposited micro/nanostructures are being successfully employed in biomedicine and environmental remediation.

1.1. Materials, shapes and fabrication techniques

Up to day, many nano- and microrobots have been developed by using single materials (e.g. metals, ceramics, polymers) but most of them have been fabricated by developing either composite materials or combining different materials within the same structure/device. The selection depends, among other things, on the mechanism responsible of the propulsion of the micro/nanostructures (see Table 1). Since the first demonstration of micromotors in 2005 [16,17], there have been significant advances in terms of fabrication, assembly and combination of materials. The idea behind is fabricating microdevices with catalytic, magnetic, electrical, optical or acoustic properties, and their combination, in order to make them move using different mechanisms -chemical propulsion (self-propulsion) or externally induced propulsion- that will be explained below. The first micromotors were based on catalytic metals like Ni [16] or Pt [17] for self-propulsion. For example, the Au-Pt system has been very employed for self-propelling bimetallic rods [17,18]. This system has taken profit of the catalytic properties of Pt for reduction of H_2O_2 to O_2 which disrupts the hydrogen bonding network of water, lowering the surface tension by the creation of a liquid-vapor interface. Because oxygen is only created in one end of the rod, an interfacial tension gradient is created along the rod length, which makes the rod propel. Not only the material(s) but also the shape and geometry are of paramount importance. Thus, the Au-Pt systems has been prepared in other simple geometries like Au spherical particles half coated with Pt (Janus particles) [19,20] or tubular structures with the Pt inside [6,21,22] (Fig. 2A). In the same way, other catalytic systems based only on metallic elements have been investigated like Ni-Au, Pd-Au, Pt-Rh, Pt-Cu and Ru-Au [18,23] (Fig. 2B). However, micromotors containing a catalytic metal coated onto polymers (e.g. polystyrene, polyaniline) [24,25] or ceramic materials (e.g. silica) [26,27] have also been investigated (Fig. 2C). Not only the materials employed but also the shape has a clear impact on the micropropeller performance like velocity or mechanism of motion.

Although the former materials are still being widely used, increasing efforts have been devoted to employ materials with the required properties/functionality to fabricate externally powered micro/nanomotors (e.g. magnetic, electric, thermal or ultrasound). Magnetically actuated micro/nanoscale structures are of particular scientific and technological interest for addressing the challenge of propulsion at the submicroscale while obviating the fuel requirement of catalytic motors and the need of changing the surrounding environment. Prove of such interest is the high number of artificial magnetic microswimmers recently published in the literature [30,44–47]. As in the case of chemical propulsion, magnetic swimmers have gone from single materials (e.g. nickel, cobalt, magnetite (Fe_3O_4),…) to multimaterials (combining metals, ceramics and polymers) (e.g. Ni/PPy, Ni/Ag/PPy, Pt/Ni/Au/Ni/Au, polystyrene/Fe_3O_4 microparticles, Ti/Fe/Pt,…) and from simple shapes (e.g. nanoparticles, nanorods, nanotubes, …) to more complex architectures (e.g. helixes, flagella-shape, microsyringes, ciliary-shape, etc…) (see Table 1 and Fig. 3) [31,48–51]. Most of the designed micromotors have been inspired from biological systems like bacteria or spermatozoa in order to achieve more sophistication onto the motion of artificial micromotors [31,50,52]. All the former parameters clearly impact on the swimming performance of the micro/nanorobots (e.g. mechanism of motion, velocity, direction, …) as it will be explained below.

Electric field is another source of energy to induce motion of micro/nanostructures via different mechanisms like electrophoresis, dielectrophoresis, electroosmosis or polarization (bipolar electrochemistry) [57]. The work of Chang et al. showed the propulsion of miniature semiconductor diodes in water when subjected to an external alternating electric field due to the conversion of the electrical energy into mechanical energy [58]. This study served as inspiration to fabricate diode nanowires motors (multisegmented nanowires) like PPy-CdS, Au-CdSe-Au, or CdSe-Au-CdSe [35,39] prepared using conducting materials (e.g. Au) and semiconductors (e.g. CdSe, PPy). Or the work of Zhang et al. that reported not only the propulsion but also the confinement and collection of SiO_2/Ti Janus particles when placed on interdigitated microelectrodes under AC applied electric fields [38]. Thus, electrically conductive materials are needed to propel microswimmers by bipolar electrochemistry. Metals or carbon-based materials have been studied [59,60] (Fig. 4).

Ultrasound and light, although less studied, have also been used as the energy source to achieve propulsion at the micro/nanoscale. Different acoustic microswimmers have been fabricated using metallic materials alone or in combination with polymers. For example, Wang *et al* synthesized segmented metallic rods (e.g. AuRu, AuPt) [40] and Li *et al* have fabricated a helical Ni coated Pd structure joined to a Au nanorod [61] while

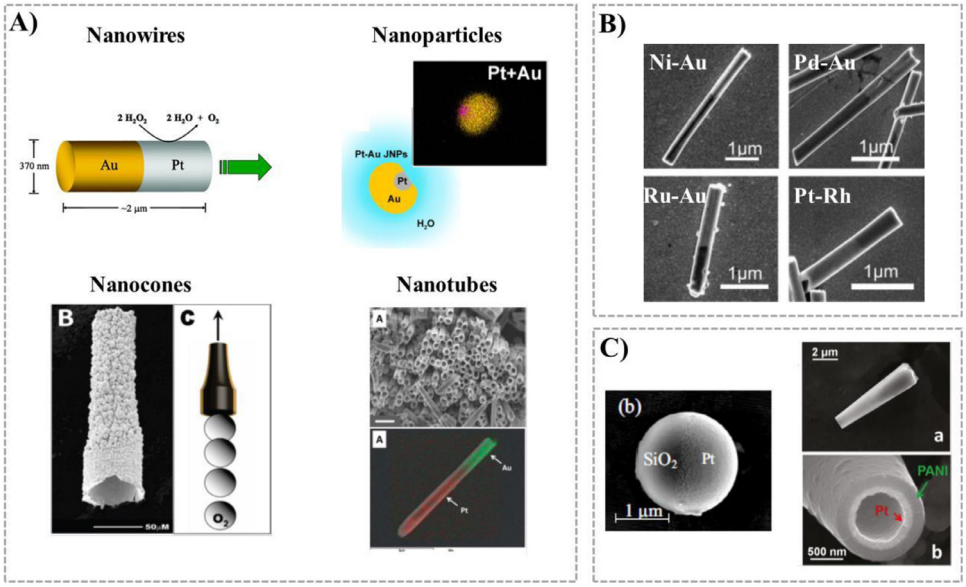

Fig. 2. Examples of self-propelled catalytic micromotors. (A) Reported Au-Pt micromotors as a self-propelled model micromotor prepared with different shapes: nanowires, nanoparticles, nanocones and nanotubes. Reproduced with permission from references [6,17,20,21]. Copyright 2013 Royal Society of Chemistry, 2004 American Chemical Society, 2014 American Chemical Society and 2010 American Chemical Society, respectively. (B) Examples of other bimetallic microswimmers (Ni-Au, Pt, Rh,…) as catalytic micromotors. Reproduced with permission from reference [18]. Copyright 2006 American Chemical Society. (C) Examples of metal-polymer and metal-ceramic materials as self-propelled swimmers. Reproduced with permission from references [25,26]. Copyright 2011 Americal Chemical Society and 2009 American Institute of Physics, respectively.

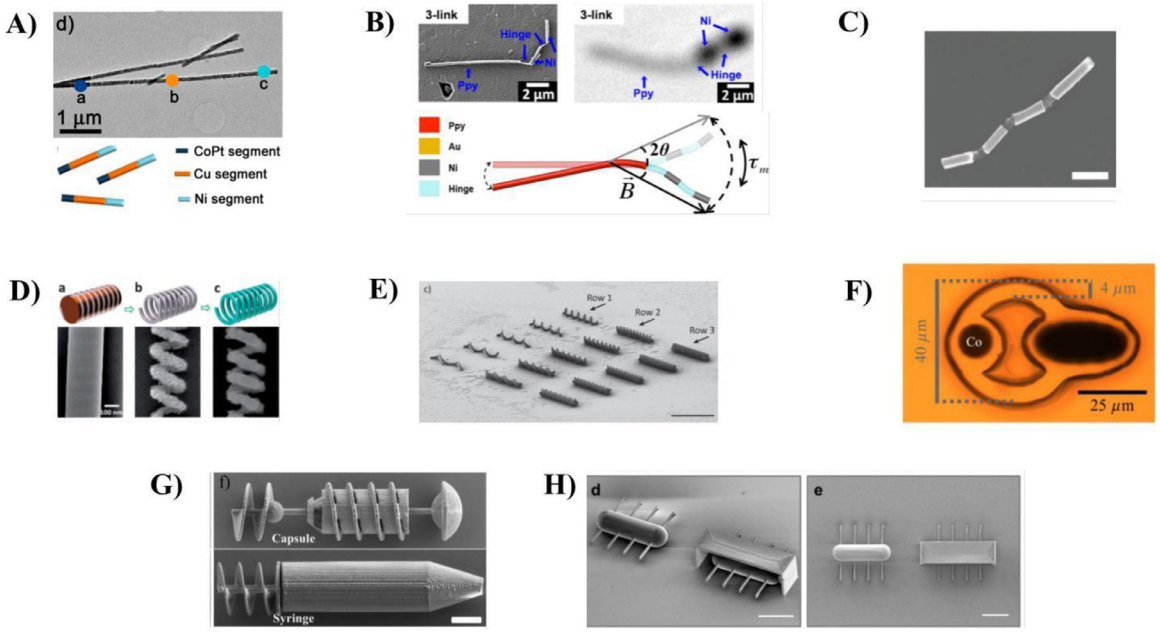

Fig. 3. Micro-nanomotors prepared using different magnetic materials and with different shapes. (A) Trisegmented CoPt/Cu/Ni nanowires prepared by templated-electrodeposition. Reproduced with permission from reference [30]. Copyright 2016 American Chemical Society. (B) Composite multilinked nanowires-based microswimmers. The swimmers are composed by an elastic polypyrrole tail and different magnetic Ni segments separated by polymeric flexible hinges. Reproduced with permission from reference [53]. Copyright 2015, American Chemical Society. (C) Multilinked micromotor composed of four segments (Au, Ni, Ni, Au) and linked by flexible silver hinges. Reproduced with permission from reference [50]. Copyright 2016, Wiley. (D) Helical nanorobots obtained using electrodeposition and dealloying. Reproduced with permission from reference [54]. Copyright 2014, Royal Society of Chemistry. (E) Array of helical microswimmers fabricated using direct laser writing from SU-8 photoresist-Fe_3O_4 superparamagnetic nanoparticle composites. Reproduced with permission from reference [55]. Copyright 2014, Wiley. (F) Magneto-elastic swimmers fabricated using photolithography and electrodeposition. The swimmers are made of soft Co and hard CoNiP ferromagnetic particles elastically linked by PDMS. Reproduced with permission from reference [34]. Copyright 2019, American Physical Society. (G) SEM image of microtransporters (microcapsules and microsyringes) fabricated with SU-8 photoresist using 3D direct laser writing and subsequent deposition of a Ni/Ti bilayer by selective physical vapor deposition. Reproduced with permission from reference [31]. Copyright 2015, Wiley. (H) Magnetic ciliary microrobots fabricated using 3D laser lithography to build the polymeric base structure and subsequent Ni/Ti metal sputtering. Reproduced with permission from reference [56]. Copyright 2016, Nature Publishing Group.

Table 1
Overview of the fabrication technique and propulsion mechanism of some reported micro/nanomotors.

Micromotor material	Fabrication technique	Propulsion mechanism	Reference
Pt/Polydimethylsiloxane (PDMS) microplates	Electron beam evaporation	Chemical propulsion	[24]
Pt/Au nanowires	Templated-based electrodeposition	Chemical propulsion	[17]
Polyaniline/Pt microtubes	Templated-based electrodeposition	Chemical propulsion	[25]
Ti/Fe(Co)/Au/Pt microjets	Electron beam evaporation + rolled-up	Chemical propulsion	[28]
Pt/silica microspheres	Sputtering + Self-assembly	Chemical propulsion	[29]
CoPt/Ni/Cu trisegmented nanowires	Templated-based electrodeposition	Magnetic propulsion	[30]
Epoxy-based photoresist (SU-8)/Ni/Ti helical microswimmers	3D direct laser writing + physical vapor deposition	Magnetic propulsion	[31]
Microswimmer composed of an helical tail (InGaAs/GaAs/Cr hybrid semiconductor-metal trilayer) and a head (Cr/Ni/Au trilayer)	Physical vapor deposition	Magnetic propulsion	[32]
Methacrylamide chitosan-Fe_3O_4 double helical Microswimmer	Two-photon direct laser writing	Magnetic propulsion	[33]
Polydimethylsiloxane (PDMS)/Co/CoPt	Photolithography + electrodeposition	Magnetic propulsion	[34]
CdS-Ppy	Templated-based electrodeposition	Electric propulsion	[35]
Pt/Polystyrene microparticles	Electron beam evaporation	Electric propulsion	[36]
Au/TiO_2 microspheres	Solvent extraction/evaporation method + sputtering	Electric propulsion	[37]
SiO_2/Ti	Electron beam evaporation	Electric propulsion	[38]
Au/WO_3/C microspheres	Hydrothermal synthesis + sputtering	Light propulsion	[39]
Au/Ru bimetallic nanorods	Templated-based electrodeposition	Acoustic propulsion	[40]
Microswimmer composed of a rod-like flagellum made of polypyrrole and a head made of Ni/Au composite	Templated-based electrodeposition	Acoustic propulsion	[41]
Ppy/Ni/PDA/Escherichia Coli	Templated-based electrodeposition + PDA assembly + incubation	Biological propulsion	[42]
PS/Fe/Escherichia Coli	Electron beam evaporation + incubation	Biological propulsion	[43]

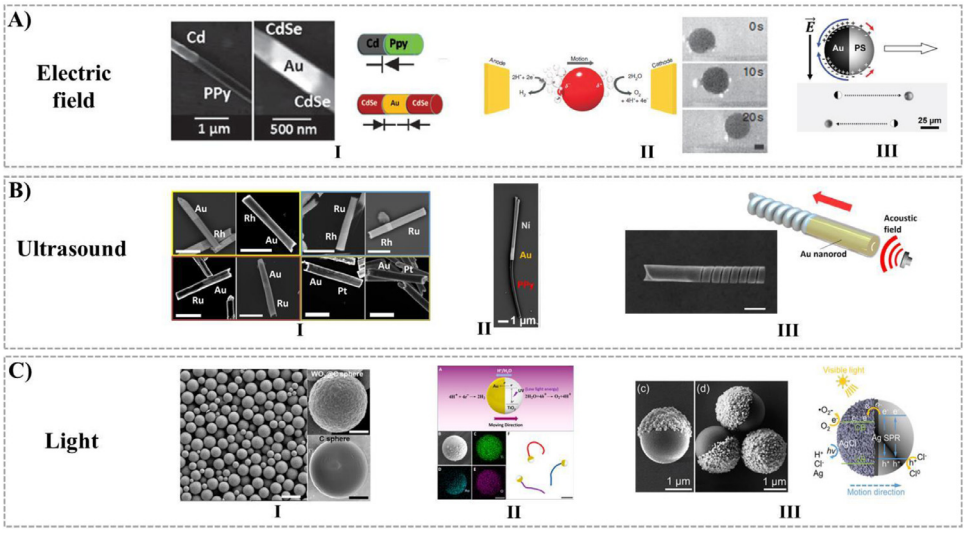

Fig. 4. Examples of micro/nanomotors propelled using different stimuli. (A) electric fields: (I) SEM image of Cd-PPy and CdSe-Au-CdSe multisegmented nanowires used as diodes for electrical propulsion and scheme showing the relationship between diode and the different materials. Reproduced with permission from reference [35]. Copyright 2010, Royal Society of Chemistry, (II) Scheme of water splitting by bipolar electrochemistry and motion of a micron-size glassy carbon sphere under an electric field. Reproduced with permission from reference [60]. Copyright 2011, Nature Publishing Group, (III) Scheme of a Janus particle motion induced by charge electrophoresis when an AC electric field is applied. Reproduced with permission from reference [36]. Copyright 2017, Wiley. (B) Ultrasounds: (I) SEM images of bimetallic nanowires after their release of the membrane used as a template during electrodeposition. Reproduced with permission from reference [40]. Copyright 2016, American Chemical Society, (II) Nanoswimmer made of a flexible PPy tail and a Ni/Au head. Applying acoustic waves generates acoustic microstreaming in water to get propulsion. Reproduced with permission from reference [41]. Copyright 2016, American Chemical Society, (III) SEM image and scheme of a magneto-acoustic micromotor formed by a Ni coated Pd helical structure and a solid Au segment. Reproduced with permission from reference [61]. Copyright 2015, American Chemical Society. (C) Light: (I). SEM images of Au-WO_3@C Janus microspheres. These particles move under UV-irradiation through a diffusiophoretic mechanism. Reproduced with permission from reference [63]. Copyright 2017, American Chemical Society. (II) Scheme, SEM and EDX images of Au-TiO_2 Janus microparticles propelled via electrophoretic mechanism due to the catalytic decomposition of H_2O under UV light. Reproduced with permission from reference [37]. Copyright 2015, American Chemical Society. (III) SEM images of PS/Ag/AgCl Janus microparticles and scheme showing the mechanism of propulsion via visible light absorption of the Janus micromotors based on the surface plasmon resonance effect. Reproduced with permission from reference [64]. Copyright 2018, Wiley.

Ahmed *et al* synthesized a two-part microswimmer composed of a PPy flexible tail and a Au/Ni metallic head [41]. A full control of the former microrobots -levitation, propulsion, alignment, rotation and self-assembly into complex architectures- was achieved by modifying the acoustic wave frequency. Another strategy was the evaporation of a biocompatible perfluorocarbon emulsion previously coated onto the microbot using ultrasounds. The release of the bubbles led to high-velocity microswimmers [62]. On the other hand, light is also another useful source of energy to propel micromotors as it shows some advantages like a control of the motion by tuning the intensity and the wavelength of the light or the wireless transmission of energy. The only requirement is that the medium

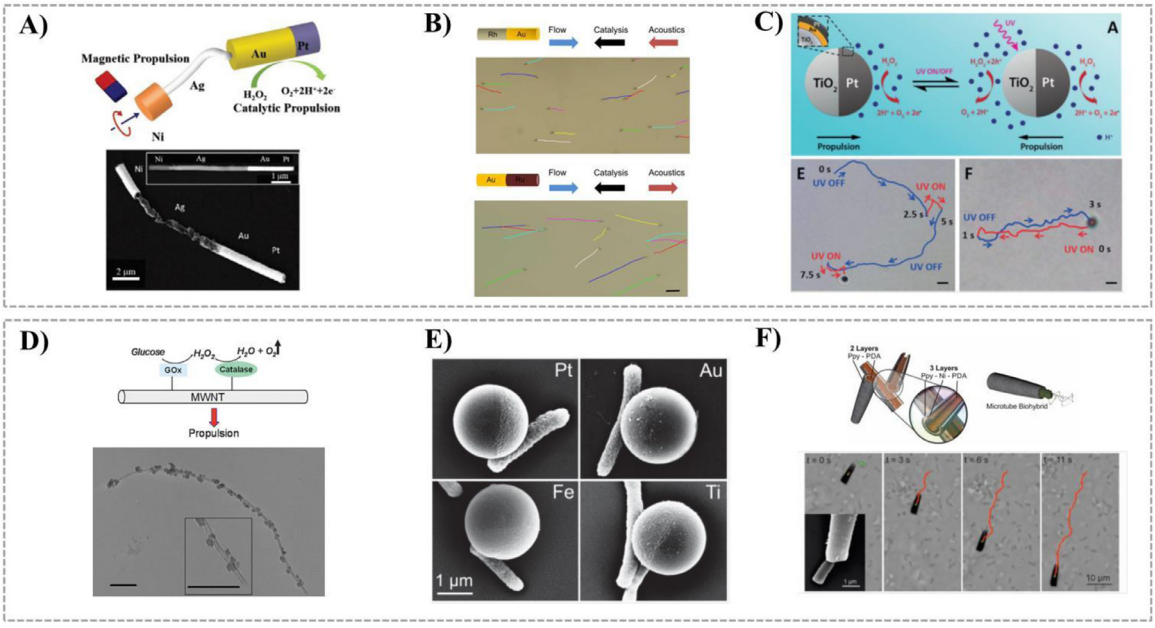

Fig. 5. Examples of hybrid micro- and nanomotors powered using at least two different power sources (Top panel). (A) Scheme and SEM image of a magnetic-catalytic micromotors composed of a Pt-Au segment and a Ni segment separated by a flexible Ag hinge. Reproduced with permission from reference [76]. Copyright 2011, Wiley. (B) Scheme of catalytic-acoustic bimetallic micromotors and their direction of their motion depending on the balance between the chemical catalysis and the acoustic forces in each micromotor. Reproduced with permission from refence [70]. Copyright 2017, American Chemical Society. (C) TiO_2/Au/Pt Janus microparticles capable of both catalytic powered motion (catalytic decomposition of H_2O_2) and light-driven propulsion (photoelectrochemical reaction onto TiO_2 semiconductor). The competing chemical reactions results in a tunable motion depending on the fuel concentration and light intensity. Reproduced with permission from refence [68]. Copyright 2018, Wiley. Examples of biohybrid micro- and nanomotors (Bottom panel). (D) Scheme and SEM image of functionalized carbon nanotubes with glucose oxidase (GOx) and catalase enabling the tandem catalytic conversion of glucose into motion. Reproduced with permission from refence [75]. Copyright 2008, Royal Society of Chemistry. (E) SEM images showing polystyrene-metal (Pt, Au, Fe, Ti) Janus particles and *E. coli* bacteria attached to them. Reproduced with permission from refence [43]. Copyright 2015, Wiley. (F) Biohybrid micromotors containing PPy-PDA or PPy-Ni-PDA and incubated with *E. Coli* to create bacteria-driven swimmers. Sequence of images showing the motion of the micromotor over time. Reproduced with permission from refence [42]. Copyright 2017, Wiley.

must be transparent to the light wavelength employed. Different light-driven motors have been prepared by partially coating either ceramic or polymeric particles (SiO_2, TiO_2, WO_3, polystyrene) with gold [37,63–66]. Different mechanism can explain their propulsion when illuminated with NIR or UV light like thermophoresis or photocatalysis but they will be explained below. Other materials have been studied (BiOI, Cu_2O, Fe_2O_3, black TiO_2) in order to use a non-harmful and more abundant radiation like visible light [67] (Fig. 4).

Finally, previous materials have been combined to fabricate hybrid micro- and nanomotors with the possibility to be powered by multiple sources aiming to expand the applications window and have a broader scope of operation (e.g. higher control of motion, better position precision and adaptability to the changing surroundings, etc). To date, several hybrid swimmers have been successfully developed including two-power sources like chemical/light [68], magnetic/acoustic [61], chemical/magnetic [69], chemical/acoustic [70] or light/acoustic [71]. For example, Gao et al. developed the first hybrid chemical-magnetic nanomotor, a multisegmented nanowire, composed of catalytic (Pt-Au) and magnetic regions (Ni) joined by thinner Ag segment to confer flexibility [69]. Or Villa et al. fabricated hybrid microrobots by decorating $BiVO_4$ star-shape structures with Fe_3O_4 magnetic nanoparticles. While Fe_3O_4 NPs enables magnetic actuation, the photoactivity of $BiVO_4$ under visible light enhances the swimming performance; thus, obtaining a magnetic/light propelled motor [15]. Moreover, other groups are focusing on incorporating more than two propulsion methods like the work of Yuan et al. where they develop Janus micromotors incorporating quantum dots, Fe_3O_4 nanoparticles and Pt or MnO_2 to respond to light, magnetic field and chemical fuel stimuli respectively [72] (Fig. 5). And other groups are preparing such hybrid nano/micromotors by combining synthetic materials with biological components (e.g. cells, enzymes), where the biological entities are essential for the propulsion of the entire biorobot. The use of the biological components has several advantages: (i) a more efficient conversion of chemical into mechanical energy, (ii) a higher sensitivity to the surrounding environment, (iii) biocompatibility and (iv) broader applicability. For example, *E. coli* bacteria have been combined with synthetic materials like PPy microtubes functionalized with polydopamine and coated with Ni [42] or Janus Fe/polystyrene (PS) microparticles [43]. In these biomotors, bacteria confer motion and the magnetic field confers directionality. Enzymes, unlike cells, do not propel the devices but they participate in chemical reactions that do induce their movement. Thus, Sanchez et al. developed a tubular micromotor with an inner gold layer coated with a self-assembled monolayer (SAM) where the catalase enzyme was bound. The enzyme catalyzed the H_2O_2 decomposition generating oxygen bubbles that induced motion. They reported that speed of the enzyme-based micromotor was 10 times higher than the same micromotor using Pt as a catalytic system [73]. Several other studies have used different enzymes like glucose oxidase (GOx) or bilirubin oxidase (BOX) [74,75] (Fig. 5).

This field has rapidly evolved and one of the main reasons is the advanced in nanoscience and nanotechnology and specially in the micro and nanofabrication techniques. Thus, researchers have been able to fabricate miniaturized mobile structures of different materials, multiple shapes and sizes ranging from tens of nanometers to several hundreds of micrometers as previously shown. Up to day, different physical, chemical and electrochemical techniques have been employed for the fabrication of the micro/nanodevices (see Table 1). The election of the technique depends on the characteristics we want to confer to the designed micromotor including types of materials and composition, their distribution, shape and properties. Several techniques have

been used like physical vapor deposition (PVD) [32], two-photon polymerization (2PP) [33,55], rolling up technology [28], glancing angle deposition (GLAD) [77,78], self-assembly [29,79], photolithography [80] or layer by layer (LbL) deposition [81,82]. Previous physical deposition techniques like conventional PVD, GLAD or 2PP have been successfully employed for the fabrication of micro/nanomotor with complex shapes and high precision. PVD technique consists on the vaporization of the target material, transported and subsequently deposited onto the substrate surface to get thin films. The vaporization step can be done by different methodologies like bombardment with ionized inert gases (e.g. argon) as in sputtering or with an electron beam in electron beam evaporation. The usefulness of this technique is that it can be used to coat nano/microstructures with varied materials in order to confer those nano/microstructures with properties like catalytic, magnetic or optic properties, among others. GLAD is a physical technique that was developed to deposit the vapor onto the substrate at grazing incidence. Changing the angle between the substrate and the vapor flux allows obtaining complex 3D structures of different materials. For example, Wu et al. fabricated helical microstructures by GLAD method using silica as the body and further coated with nickel to confer them with magnetic properties [83]. Moreover, PVD techniques are widely used to confer asymmetry to the motors as the material can be selectively deposited on only one side of the microstructures. Zhao and co-workers showed how to selectively deposit different metallic layers (Ti, Au, Ni) onto silica microbeads [84]. However, PVD methods have some disadvantages like the need of high vacuum and high temperature conditions, slow deposition rates or the need to place an array of ordered seeds on the substrate to fabricate the micromotors making these techniques expensive and time consuming. While those techniques have been mainly used for metallic coating, 2PP method, a direct laser technique, is used to prepare complex 3D polymeric micro/nanostructures (e.g. helices) with high resolution. In this technique, the laser impacts a certain region of a photosensitive resist that undergoes polymerization by activating photo-initiators in the resist. The non-polymerized resist can be washed out to get the 3D micro/nanostructures. Huang and coworkers developed microcapsules and microsyringes fabricated with SU-8 photoresist using photon polymerization and subsequently covered with Ni/Ti bilayer to confer with magnetic properties [31]. Or more recently, Cabanach et al. have successfully fabricated hydrogel-based helical microrobots using zwitterionic non-immunogenic photoresists to avoid their detection and phagocytosis by macrophages [85]. The main 2PP drawbacks are complex equipment, large waste of material or its limitation to get mainly polymeric structures. On the other hand, assembly methods like LbL are a versatile strategy to obtain micro/nanomotors through the spontaneous reorganization process of different layers with opposite charge. The reversibility of the process and the noncovalent interaction make this methodology very attractive to assemble and disassemble the building blocks of the micromotors that can be as varied as small organic molecules, inorganic compounds, macromolecules or colloids. For example, magnesium microparticles coated with subsequent Au, alginate and parylene layers were synthesized following this LbL methodology to be photoacoustically propelled towards target regions in intestines [82]. The need of rinse steps between subsequent layer deposition to remove weakly adsorbed polyelectrolytes and avoid cross-contamination make this technique time consuming. Electrodeposition has been, by far, the technique most often employed [61,86,87]. As explained in greater detail below, electrodeposition offers numerous advantages compared to earlier techniques. These advantages include (i) a wide variety of materials (metals, polymers, ceramics) in different sizes (from nanometers to micrometers) and shapes (films, wires, helices, etc.) that can be electrodeposited; (ii) good resolution; (iii) simple set-up; (iv) easier operating conditions (i.e., room temperature and atmospheric pressure without requiring a vacuum system); (v) lower cost (simplicity of set-up and normal laboratory conditions compared to previous techniques significantly reduce costs and energy consumption); (vi) mass production; and (vii) scalability. This technique fulfills desired factors including low cost, scalability, and manufacturability and, thereby, has the potential to reduce the costs of producing micro/nanomotors in the near future. For a more complete overview of the fabrication techniques employed in micromotor fabrication, the authors recommend two references [88,89].

1.2. Functionalization and modification of robot properties

Chemistry is another discipline widely involved in the micromotors field. Incorporation of new functionalities to the micro/nanodevices is of key importance as new properties can be conferred and therefore the ban of applications is significantly enlarged. One strategy is the functionalization of the devices with (bio)molecules (e.g. drugs, DNA, peptides and proteins, etc.) as it can be useful for many purposes like transport and delivery of drugs, conferring biocompatibility, sensing ability, recognition of certain cells or antibodies, improving photodynamic therapy or enhancing photocatalytic degradation of pollutants [90–95]. A second strategy is coating some parts of the swimmers with non-cytotoxic materials. For example, nickel is a ferromagnetic metal widely employed in the fabrication of magnetic nanomotors. However, its cytotoxic effect hinders its use in biomedical applications. For this reason, different strategies have been followed to cover it like superficial oxidation to give biocompatible NiO or coating nickel with noble metals like gold or platinum [96,97] (Fig. 6). Finally, the integration of stimuli-responsive materials is a very interesting approach to get intelligent micro/nanodevices able to react to either changes in the surrounding environment (e.g. pH, temperature) or external power sources. For example, Chen et al. fabricated core-shell Fe-SiO_2 nanocapsules loaded with an anticancer drug and a MRI contrast agent and covered with multiple polyelectrolyte layers of poly-L-lysine and sodium alginate to control the drug release as a function of pH [98]. The polyelectrolyte layer allowed the release of the drug at pH = 5 in contrast with pH = 7.4. At the slightly basic pH, the carboxyl groups of alginate and the amine groups of poly-L-lysine are ionized meaning an electrostatic attraction between both polymers thus preventing the drug release. On the other hand, Buzuyuk et al. recently reported a magnetically powered helical microrobot able to deliver a drug by light stimulation. The robot was fabricated using methacrylamide chitosan blended with superparamagnetic iron oxide nanoparticles as the photosensitive and magnetic materials respectively. While locomotion was achieved applying magnetic field, light was used to release the previously encapsulated drug into the polymer [33].

1.3. Small-scale propulsion

One of the most exciting aspects of small-scale robotics is looking for new locomotion mechanisms and incorporating strategies for a better control of the micro/nanorobots motion (e.g. speed, direction, velocity). Basically, micro/nanomotors converts energy into movement and force. However, propelling objects with sizes of the order of micrometers or lower in liquid is not an easy task as motion at low Reynolds number is dominated by Brownian collisions, viscous forces -over inertial ones- and some other surface phenomena. Overall make such devices as if they were in a highly “viscous” medium making motion very difficult. The Purcell’s scallop theorem states that no net translation is possible at such length scales when reciprocal motion exists, that is, when the swimming motion is symmetric with respect time reversal, like

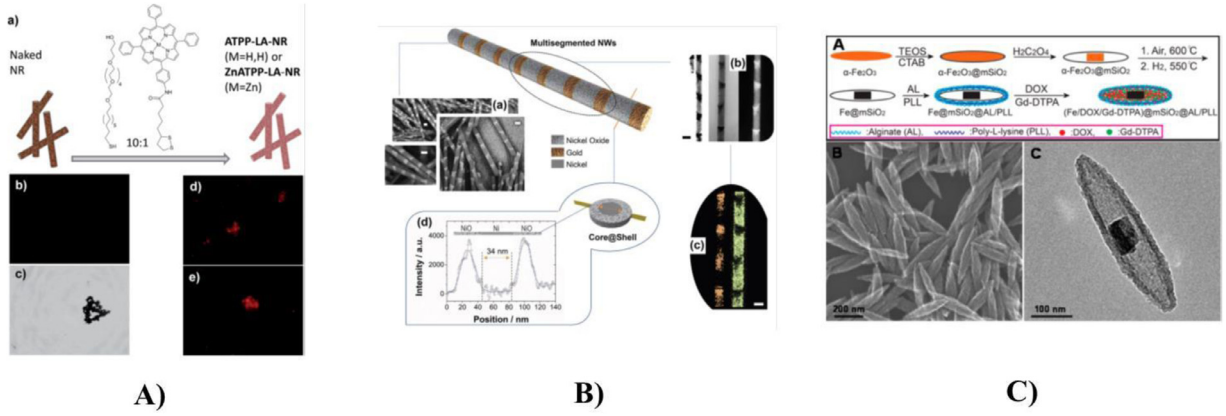

Fig. 6. Functionalization strategies employed to modify the surface of micro/nanomotors. (A) Scheme showing the functionalization of nanorods with porphyrins and Zn-containing porphyrins for photodynamic therapy. And fluorescence microscope images showing functionalized and non-functionalized nanomotors. Reproduced with permission from refence [92]. Copyright 2017, Royal Society of Chemistry. (B) Oxidation treatment of Ni segments in multisegmented Ni-Au nanorods to confer biocompatibility through the formation of nickel oxide surface layers. Reproduced with permission from refence [97]. Copyright 2018, Wiley. (C) Magnetic nanocapsules consisting of an hematite core and a mesoporous silica shell containing doxorubicin as a model drug. The capsules were functionalized with multiple polyelectrolyte layers of poly-L-lysine and sodium alginate to thigh drug delivery control. Reproduced with permission from refence [98]. Copyright 2014, American Chemical Society.

the valves opening and closing mechanism of the scallop when swimming at low Reynolds numbers. Therefore, to overcome such limitations microswimmers must nonreciprocally deform with time to get a net displacement of the micro/nanoobjects [99]. Up to day, various propulsion strategies have been developed to overcome the constrains of Purcell's theorem and therefore to power micro/nanoswimmers. These strategies can be classified as: (i) chemical propulsion (or self-propulsion), (ii) external propulsion, and (iii) a hybrid strategy that involves both [100] (Fig. 7). Particular attention has been given to self-powered micromotors based on the asymmetric catalytic decomposition of fuel molecules containing solution onto the micro/nanoobjects surface. Janus microstructures facilitate the local or asymmetric decomposition of the fuel generating either surface tension, concentration or field gradients that, in turn, create imbalance of forces and therefore flow. Thus, chemical energy is converted into kinetic energy. For example, bisegmented Au-Pt nanowires are self-propelled by the electrocatalytic decomposition of H_2O_2 fuel thanks to the self-electrophoretic mechanism. While the reduction of H_2O_2 takes place in the gold segment ($2H_2O_2 + 2H^+ + 2e^- \rightarrow 2H_2O$), the oxidation of the fuel O_2 happens in the platinum segment ($2H_2O_2 \rightarrow O_2 + 2H^+ + 2e^-$). The asymmetric bubble generation and the proton concentration gradient along the wire causes motion [17,18]. The micromotor speed is dependent on the fuel decomposition rate which is dependent on the concentration solution (higher concentration higher velocity) but also on the micromotor composition. Thus, micromotor speed was dramatically increased when the Au segment was substituted by the Au-Ag alloy [101] or the Pt segment was replaced by carbon nanotube (CNT)-doped Pt [102]. Such improvement is attributed to the higher catalytic efficiency of the Au-Ag or CNT-doped Pt materials towards H_2O_2 reduction and oxidation respectively.

However, this strategy usually requires fuels such as hydrogen peroxide (H_2O_2), hydrazine (N_2H_4), bromine (Br_2) or iodine (I_2), which are highly cytotoxic avoiding their use for biological applications. However, some alternative fuels have been recently reported like calcium carbonate and tranexamic acid (microparticles made of calcium carbonate and tranexamic acid can swim through blood by carbon dioxide bubble propulsion) or glucose [103,104]. Although self-propulsion is very attractive, this strategy shows some drawbacks like (i) lack of directionality, (ii) toxic chemicals and (iii) continuous external fuel supply that hinder the use of these self-fuelled micro/nanomachines for biomedical applications. For more details on the mechanism of self-powered microrobots, see the following references [105,106].

To avoid the previous limitations, externally powered micro/nanomotors have been developed. Thus, external propulsion includes the use of energy mainly coming from magnetic and electric fields, light and acoustic fields. Magnetic fields are of particular interest as they have been very extensively studied because its advantages: (i) non-invasive, (ii) no harmful to living organism, (iii) non-absorbed in fluids so can penetrate living organisms including the human body and (iv) remote control of microrobots [107]. However, overcoming the lack of inertia at low Reynolds number is essential to get motion of the micro/nanostructures. Different strategies have been designed requiring nonreciprocal motion, that is a mechanism that breaks the symmetry of the microrobots motion. One strategy is to apply inhomogeneous or time-varying magnetic fields (e.g. rotating, oscillating, …) and a second strategy is to design microstructures that change shapes by following an asymmetric time sequence. Regarding the first strategy, helical microrobots have been deeply investigated by many research groups. Thus, the group of B. Nelson at ETH Zurich was the first to demonstrate the swimming of helical robots under rotating magnetic fields. These robots, inspired by the motion of bacteria through the rotation of their flagella, consisted of a Cr/Ni/Au magnetic head and a helical tail composed of a InGaAs/GaAs bilayer. With this architecture, the direction of the micromotor was controlled with the direction of the applied rotating field [32]. Since then, many research groups have developed similar structures like the group of J. Wang who fabricated Pd-Ni helical nanorobots by a three-step process: template-assisted electrodeposition of Pd-Cu, etching of Cu and creating a thin Ni film by evaporation [108] or Kim's group who fabricated Co and CoFe nanosprings by electrodeposition [109]. All those micromotors were able to move in water under rotating magnetic fields. On the other hand, more complex microdevices -micropumps, microsyringes- have been prepared but with the same mode of operation: applying rotating magnetic fields to propel them [31]. Regarding the second strategy, flexible microstructures have been fabricated that change shapes in an asymmetric time sequence. For example, Li et al. fabricated a multilink two-arm nanomotor with a central gold segment and two nickel arms connected to it by flexible silver hinges. The Ni-Ag-Au structures were actuated by applying a planar oscillating magnetic field. In response to this field, the two Ni arms move cooperatively to push the central Au segment forward [110]. A second

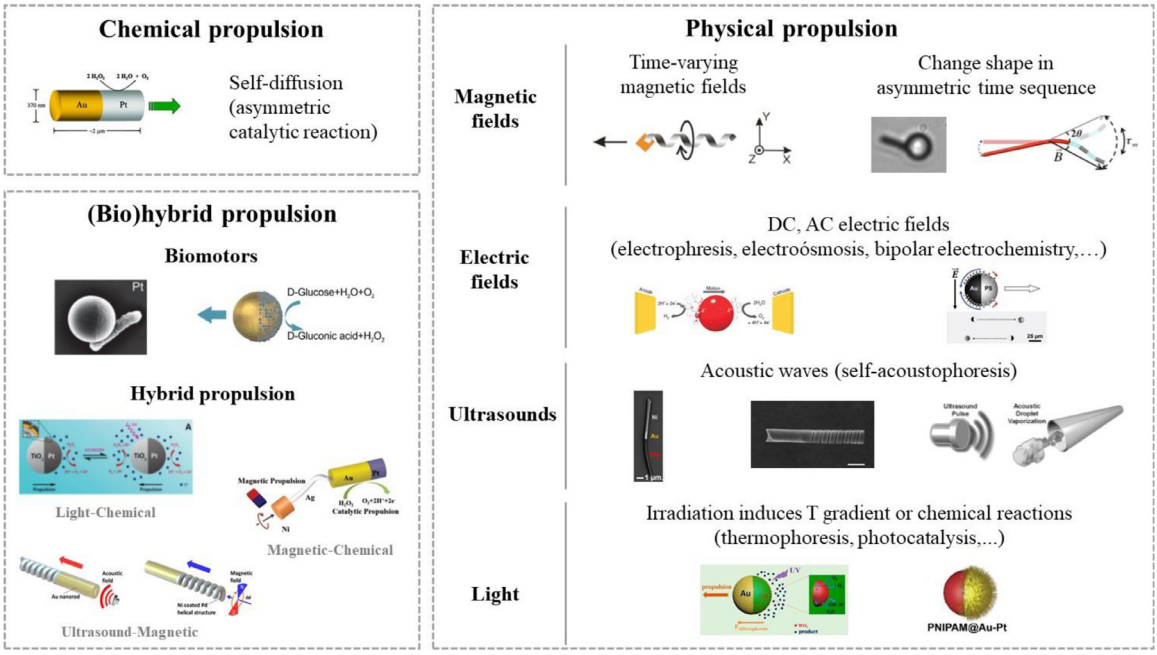

Fig. 7. Propulsion mechanisms of micro/nanomotors. Chemical propulsion: The asymmetric chemical reaction in Au-Pt bisegmented micromotors induces their propulsion. Reproduced with permission from reference [6]. Copyright 2013 Royal Society of Chemistry. Physical propulsion methods include: (i) Magnetic fields: (Left) Helical microswimmer consisting on a helical tail resembling a bacterial flagellum and a soft-magnetic head on one end. Reproduced with permission from reference [32]. Copyright 2009, American Institute of Physics. (Center) Microswimmer formed by the magnetic self-assembly between a Ni nanorod and a superparamagnetic polystyrene-Fe_3O_4 sphere. Reproduced with permission from reference [79]. Copyright 2018, Nature Publishing Group. (Right) Composite multilinked nanowires-based microswimmer composed by an elastic polypyrrole tail and different magnetic Ni segments separated by polymeric flexible hinges. Reproduced with permission from reference [53]. Copyright 2015, American Chemical Society. (ii) Electric fields: (Left) The applied electric field causes water splitting by bipolar electrochemistry and motion of a micron-size glassy carbon sphere. Reproduced with permission from reference [60]. Copyright 2011, Nature Publishing Group, (Right) Motion of a Janus particle induced by charge electrophoresis when an AC electric field is applied. Reproduced with permission from reference [36]. Copyright 2017, Wiley. (iii) Ultrasounds: (Left) Acoustic waves generate acoustic microstreaming in water to get propulsion of nanoswimmers made of a flexible PPy tail and a Ni/Au head. Reproduced with permission from reference [41]. Copyright 2016, American Chemical Society. (Center) SEM image of a micromotor formed by a Ni coated Pd helical structure and a solid Au segment propelled by acoustic waves. Reproduced with permission from reference [61]. Copyright 2015, American Chemical Society. (Right) Acoustic waves provoke the vaporization into droplets of perfluorocarbon molecules adsorbed into the inner layer of microtubular swimmers inducing their propulsion. Reproduced with permission from reference [62]. Copyright 2012, Wiley. (iv) Light: (Left) Au-WO3@C sphere Janus micromotors propelled using UV light. Reproduced with permission from reference [63]. Copyright 2017, American Chemical Society. (Right) Thermoresponsive PNIPAM brush functionalized Au-Pt Janus micromotor capable of changing the direction of motion with the change of temperature. Reproduced with permission from reference [118]. Copyright 2019, Wiley. (Bio)hybrid propulsion: (i) Biomotors: (Left) SEM images showing polystyrene-metal (Pt, Au, Fe, Ti) Janus particles and *E. coli* bacteria attached to them. Reproduced with permission from refence [43]. Copyright 2015, Wiley. (Right) Self-propelled mesoporous SiO_2 Janus nanomotors powered by the biocatalytic reaction of the glucose oxidase enzyme. Reproduced with permission from refence [104]. Copyright 2015, American Chemical Society. (ii) Hybrid propulsion: TiO_2/Au/Pt Janus microparticles capable of both light-driven propulsion (photoelectrochemical reaction onto TiO_2 semiconductor) and catalytic powered motion (catalytic decomposition of H_2O_2). Reproduced with permission from refence [68]. Copyright 2018, Wiley. Magnetic-chemical powered micromotors composed of a Pt-Au segment and a Ni segment separated by a flexible Ag hinge. Reproduced with permission from reference [76]. Copyright 2011, Wiley. Ultrasound-Magnetic propelled micromotor formed by a Ni coated Pd helical structure and a solid Au segment. Reproduced with permission from reference [61]. Copyright 2015, American Chemical Society.

example is reported by Jang et al. on the undulatory locomotion of multilink microswimmers. They are composed of an elastic polypyrrole tail and two rigid magnetic Ni segments separated by flexible polymeric links. The microswimmer was actuated with an oscillatory magnetic field that caused net motion due to the bending of the PPy tail during each stroke breaking the symmetry of the motion with time. A high degree of deformation during motion is observed as a consequence of a time-dependent difference in the orientation of the two Ni regions [53]. The group of F. Ogrin reported the fabrication of a microswimmer made of a magnetically hard Co-Ni-P ellipsoidal particle and a soft Co spherical particle elastically linked by an elastomer. The microswimmers are also propelled by an oscillating magnetic field. The dipolar interaction between the soft and hard ferromagnets, the elastic deformation and the hydrodynamic interaction can explain the motion of the micromotor [34].

More recently, micromotors fabricated by self-assembling different pieces/structures is having more interest in order to have more flexibility, and definitely, more degrees of freedom. Thus, Garcia-Torres et al. developed a two-particle microrobot composed of a paramagnetic sphere and a ferromagnetic nanorod, that can be easily controlled by an oscillating magnetic field. Thus, the external field induces repulsion and attraction forces between both elements leading to a net translation motion. Moreover, depending on the frequency and intensity of the applied magnetic field the micromotor can change direction as a result of two interchangeable mechanisms that arise upon balancing magnetic interactions, gravity and hydrodynamics [79]. A different propulsion mechanism can be achieved when a static magnetic field is superimposed to the previous oscillating field. The resulting swinging magnetic field allows motion of the microswimmer as a result of a periodic relative movement of the two elements: the nanorod rotates and translates on the microsphere surface. As these two movements are uncoupled, the micropropeller has two degrees of freedom allowing net motion [111,112].

Electrical fields are another power source that is attracting interest in the micromotors community to propel them. DC and AC electric fields as well as homogenous and heterogeneous fields can be used to move objects at the sub-microscale under different phenomena: electrophoresis, dielectrophoresis, electroosmosis or polarization effect (bipolar electrochemistry). Although propulsion of objects was demonstrated by Velev's group in millimeter-size diodes [58], soon after different research groups successfully miniaturized such diodes to the micro- and nanoscale. For

example, PPy-Cd diode nanowires were fabricated by template-electrodeposition and actuated under a uniform AC electric field. Those nanowires moved parallel to the field axis as a consequence of a local electroosmotic flow generated. The rectification of the applied AC field induces a DC voltage between the diode electrodes. Since only half of the AC electric field cycle results in electrical current in one direction through the diode, the induced charges on the diode also move in that direction, generating the electroosmotic flow and the net motion [35]. Another strategy is the so-called bipolar electrochemistry that is based on the polarization of conducting materials under a strong applied electric field. Thus, cathodic and anodic areas are generated at the opposite ends of the microstructure triggering oxidation and reduction reactions in the corresponding areas. These spatially separated reactions imply the asymmetric generation of gas bubbles like H_2 from the reduction of water allowing micromotor's motion [60]. The motion can even be improved by adding a sacrificial material or compound (e.g. hydroquinone) which is easily oxidized as it has a lower standard potential than H_2O/O_2 and therefore suppresses O_2 formation [113].

Ultrasound is another biocompatible power source with potential applicability in the biomedical field because such high-frequency sound waves (> 20 kHz) have no deleterious effects on biological systems [114]. Several ultrasound-powered micromotors have been reported up to day. For example, Wang et al. reported that metallic nanorods (either single metallic (Au, Ru, Pt) or bimetallic (AuRu, AuPt NRs) can levitate, rotate, propel and assemble into standing waves at different frequencies. Thus, the micromotors were unidirectionally propelled (with the long rod axis parallel to the direction of motion) at speeds around 200 μm s^{-1} at the resonant frequency. The proposed mechanism is based on a locally induced pressure gradient, attributed to the shape asymmetry of the nanorod, that leads to a net translational motion by a self-acoustophoresis mechanism [40]. The same research group also demonstrated that Au-Ru-Ni nanorods can be assembled into more complex geometrically regular dimers, trimers and higher multimers at a frequency of 4 MHz. The assemblies can also be propelled by ultrasound but each assembly exhibiting a different mode of motion. As the propulsion is in a fluid, drag forces tended to break the symmetry of the structures which was favored by the non-linked nanorods (they are magnetically self-assembled) allowing deformation [115]. Later, they also showed the effect of acoustic actuation onto star-shape gold particles dynamics. Although they mainly achieved rotation of these particles, translational motion was also observed under certain circumstances. They attributed it to the spatial heterogeneity of the acoustic field. However, the mechanism is still unclear [116]. On the other hand, Ahmed et al. developed micromotors, composed of a long polypyrrole segment (e.g. flagellum) and a Ni/Au head, that where propelled using acoustic waves. The difference with the previous works is that the micropropeller was actuated by travelling acoustic waves instead of standing waves, which they claim is a better strategy since there is no effect of the chamber in the former. They attributed the motion to the force generated as a consequence of a linear and nonlinear interaction of the swimmer with the acoustic waves [41]. Another ultrasound-based strategy consists on the droplet vaporization of biocompatible perfluorocarbon chemicals bounded to the inner layer of a microtubular swimmer. The generation of bubbles leads to a high-velocity micromotor (6 m s^{-1}) with a very efficient motion. Although the mechanism is not yet understood, the authors hypothesize that the bubbles oscillation and the microstreaming around them generate the propulsion force [62].

Light is also under investigation as a power source for micro/nanomotors propulsion because it possesses several advantages like wireless transmission of the energy or fine control of the beam size (it can be reduced to the sub-micrometer range) allowing selective manipulation of micromotors and also good temporal and spatial resolution. Light allows the propulsion of microrobots by inducing either changes in temperature (thermophoresis) or chemical reactions (photocatalysis) on certain areas of the swimmers [65,66]. It has been reported that Janus microstructures like Au-SiO_2 particles can induce a temperature gradient around their surfaces when illuminated with NIR or UV light as a consequence of the different absorption energies between Au and the metal oxide [117]. The observed asymmetric temperature distribution, which is based on the surface plasmon resonance effect of gold (negligible in metal oxides), leads to the thermophoretic propulsion of the particles. This mechanism allows stopping and reinitiating the propulsion by applying an On-Off signal. Coating Janus particles with thermoresponsive polymers (e.g. poly(N-isopropylacrylamide (PNIPAM)) also allows controlling direction of motion of the micromotors [118]. In the same way, a catalytic reaction can be selectively induced in given areas of the microswimmer (only in the photocatalytic material) generating byproducts like gas bubbles, allowing their propulsion. Photocatalytic-propelled robots show the same propulsion mechanisms as those previously explained for self-propelled micromotors like self-electrophoresis, self-diffusiophoresis or bubble propulsion. For example, TiO_2 nanoparticles half-coated with Au showed photocatalytic motion. Under UV illumination, water oxidation took place selectively onto the photocatalytic TiO_2 allowing bubble propulsion. Other photocatalytically propelled motors are Au/WO_3 on carbon microspheres or Au/TiO_2 particles [37,63].

Finally, (bio)hybrid micromotors have also been successfully explored by combining different strategies of propulsion into the same microswimmer or combining them with biological systems. In the case of the biomotors, the biological system contributes with either motion (e.g. bacteria) or with a chemical reaction (e.g. enzymes). Except for the case of motors propelled by the organism, the other mechanisms are those previously explained. For detailed information on the different propulsion mechanisms, the authors refer the reader to recent published reviews [36,119–123].

1.4. Actuation and tracking of micro/nanomotors

As it has been stated at the beginning of this review, the final aim of these micro/nanomotors is realizing complex and autonomous tasks at the micro/nanoscale. The main applications foreseen for these devices are related to the health and environment sectors. For example, they are expected to have potential applicability in the biomedical field in cancer treatment (e.g. brain, pancreas), neurological diseases (e.g. Alzheimer, Parkinson), circulatory system (e.g. plaque, coronary artery disease, heart disease), kidney stones, dentistry (e.g. tooth repair) or targeted drug delivery [124–128] but also for environmental applications like water remediation (e.g. degradation of organic pollutants, recovery of heavy metals), exploration of subterranean geophysical formations or oil retrieval [129–131]. It implies that these machines must move in complex media not only in the human body through fluids -blood, saliva, urine- or tissues and organs -gastrointestinal tract, brain matter, kidney- but also in other environments like highly contaminated water, soil or oil. Due to the difficulty of the micromotors to be propelled in realistic biological environments, most of the papers published in this field have used typically Newtonian fluids for their simplicity. However, several research groups have been reported how this micromotors behave in different complex media like cells, blood or tissues. For example, Serrà et al. reported the electrochemical fabrication of Au/Ni(NiO) multisegmented nanowires [97] or Wang et al. reported the fabrication of Au nanorods [132]. Both works internalized the nanomotors into

HeLa cancer cells and actuated them inside the cells by magnetic and acoustic fields respectively, providing a new method to manipulate cells at subcellular level. Other studies have reported the actuation of micromotors at tissue level like the work of Xi et al. that successfully internalized magnetic microdrillers prepared by rolling up trapezoidal Ti/Cr/Fe membranes into a pig liver [133] or Esteban-Fernández de Ávila et al. that reported an effective in vivo drug delivery for the treatment on an stomach infection. They showed how a drug-loaded magnesium microswimmer was successfully propelled in a mouse stomach enabling an effective delivery of the drug and leading to a significant reduction of the bacterial infection [134].

However and before reaching real applications, other issues need to be addressed like those related to the set-up for micromotors motion control in real scenarios but specially/and also the techniques used for tracking of these structures in the different media. Among the different engineering strategies developed to facilitate micromotors motion control, magnetic steering has been the most developed and promising [107]. Although only a few in vivo examples have demonstrated its feasibility, recent advances show that micromotors can be wirelessly controlled in the body [123,135]. On the other hand, tracking the tiny structures is another important issue still unresolved although interesting advances are being made. For example, strategies like magnetic resonance, optical or ultrasound imaging are being investigated. All of them show advantages and disadvantages that makes them useful for certain applications. Recent studies on in vivo imaging demonstrate the potential of different strategies.

Thus, further developments in actuation and imaging technologies are essential to perform all the envisioned tasks of micromotors in a more specifically and safer manner in real scenarios. The authors refer readers to comprehensive reviews on swimming in complex media, control and tracking of micromotors [12,13,122,136]. Summarizing, there is an interrelation between propulsion mechanism-applications-materials-fabrication technique-structure-properties.

2. Basics of electrochemical synthesis of 1D nanostructures

Currently, the synthesis of micro/nanostructures is a fundamental topic in research on electrochemical deposition due to its potential application in biomedical, environmental, chemical, and, above all, electronics applications [137–140]. Although the use of electrochemical deposition was once limited to obtaining decorative metallic films or surfaces with improved resistance to corrosion, its application in the past three decades has been greatly extended into other fields. Because it allows users to control the composition, properties, thickness and shape of materials, electrochemical deposition now even competes with methods such as physical vapor deposition [137–140]. Due to its simplicity (i.e. simple experimental set-up and non-vacuum conditions required), low cost, scalability and manufacturability, electrochemical deposition also seems able to meet the financial, environmental and temporal restrictions imposed by society. Electrochemical deposition can involve various techniques (e.g. electrodeposition, electrophoretic deposition and electroless deposition) for depositing various combinations of metals, alloys, semiconductors and polymers [137,139–142].

2.1. Electrodeposition

Electrodeposition entails other processes such as electroforming, electrorefining, electrowinning, electroanalysis, electroplating, electro-precipitation and electropolymerization. Electrodeposition is chiefly used to deposit metals and alloys, which involves reducing metal ions from aqueous, organic, fused-salt or ionic liquids electrolytes [137,140,141,143]. The formula in Equation 1 represents the reduction of metal ions:

$$M^{n+}_{(aq)} + n\ e^- \rightarrow M_{(s)} \quad (1)$$

In the process represented by the formula, n electrons are provided by an external power supply. Electrodeposition is a complex, heterogeneous process that occurs in the region of electrode–solution interface, in which metal ions present in a solution are reduced to coat a conductive or semiconductive substrate with the application of an external electric field. To control the structure and properties of deposited materials, especially at the nanometric level, is essential to understand the metal–solution interface as the locus of deposition, along with the kinetics and mechanisms of the process as well as the nucleation and growth processes of the metal lattice, M(s) [137,140,143].

The simplest version of electrodeposition requires three elements: an electrochemical bath containing the metallic ions to be electrodeposited and other additives, electrodes (i.e., cathodes and anodes) and a system that provides a difference of potential or current, either constant or variable that should allow the control of the magnitude applied [137]. Reduction occurs at the cathode or, in a three-electrode system, at the working electrode, which could be a conductive or semiconductive material; by contrast, oxidation occurs at the anode or, in a three-electrode system, at the counter or auxiliary electrode. Cathodic deposition is the more popular process, primarily because many metal ions are positive, whereas anodic deposition is less often used, because it generally offers low adhesion and lacks stoichiometry [137,140].

In the last three decades, the electrodeposition of semiconductors such as ZnO or MnO_2 and polymeric coatings has also become relevant, especially for synthesizing complex 1D micro- and nanostructures for biomedical, energy and environmental applications. Such processes are also referred to as electrodeposition, because the amount of deposited material can be controlled via the charge applied through the electrodes [144]. In the case of semiconductors, electrodeposition processes are based on the electroprecipitation of metallic ions due to the formation of hydroxyl ions or highly reactive radicals—for example, the superoxide ion $O_2^{-\cdot}$—on the cathode. In the case of polymers, the formation of highly reactive radicals or the oxidation of monomers induces polymerization, which causes the deposition of the polymeric coating on the surface electrode [144,145].

Unlike other techniques for micro/nano-motors fabrication, electrodeposition has proven to be a versatile method that allows the fabrication of shape-controlled micro- and nanomaterials for use as micro- and nanomotors (Fig. 8). More specifically, electrodeposition facilitates the fabrication of such materials by using hard templates that allow the creation of exact negative replicas of the templates used. Since the introduction of such shape-controlled electrodeposition, different types of templates have been created, both related and unrelated to the polycarbonate or alumina membranes, that allow the electrosynthesis of nanowires of metals, semiconductors and polymers with different dimensions, nanotubes, micro-helices, interconnected networks of nanostructured nanomaterials such as nanocones and other incredible shapes. By extension, hard-template electrodeposition can be combined with soft-template systems, soft lithography and colloidal lithography, among others, that permit the formation of complex, multicomponent architectures with different morphologies, properties and architectures [137,140,141,143,146]. Consequently, new cooperative and synergetic means to synthesize nanomaterials based on electrodeposition are possible in nanofabrication. The electrodeposition of metals, alloys and oxides is the most important and realistic process in terms of reproducibility,

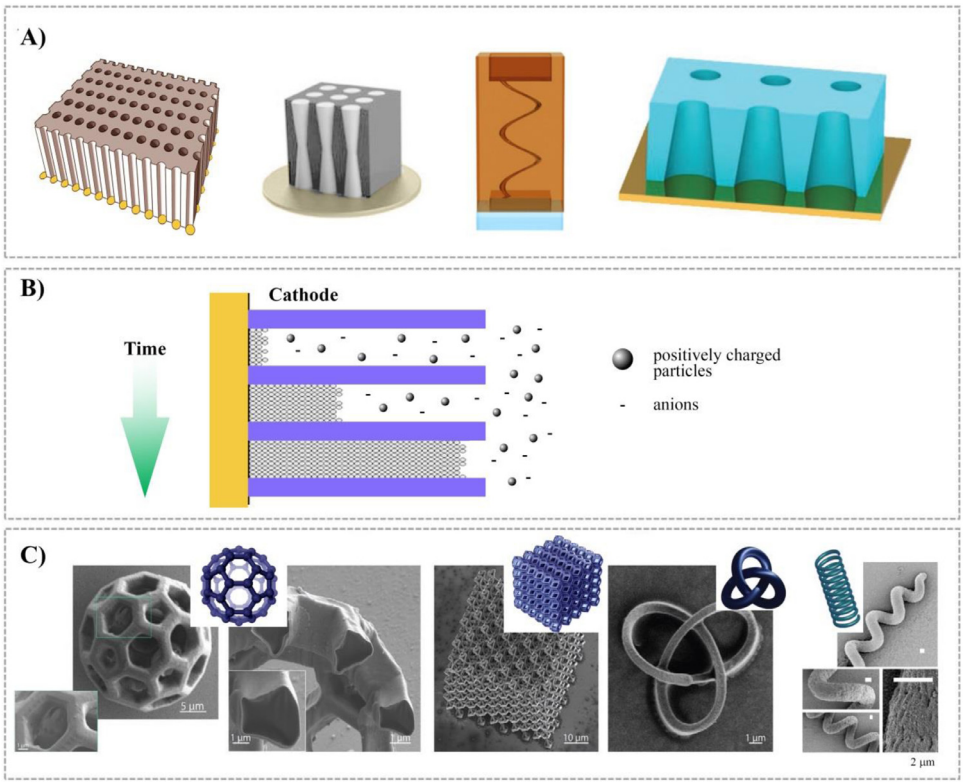

Fig. 8. (A) Examples of different hard templates used for electrodepositing micro- and nanomotors. Adapted with permission from [147,[148]. (B) Schematic representation of the electrophoretic deposition of nanowires. (C) FE-SEM micrographs of different polymeric or organic templates used for fabricating micro- and nanostructures via electroless deposition. Adapted with permission from [149,[150].

simplicity and scalability for the electrosynthesis of micro- and nanomotors [140,141,143,146].

2.2. Electrophoretic deposition

Electrophoretic deposition is a multistep process based on the deposition of charged micro- or nanoparticles suspended in a liquid on the surface of electrodes when a DC electric field is applied. In that process, nanoparticles are moved and deposited on the electrode of the opposite charge under the application of DC fields [142,151,152]. The agglomeration of micro- or nanoparticles needs to be subjected to an additional posterior process such as sintering in order to improve their integrity and robusticity. In general, the use of electrophoretic deposition is restricted to ceramic and polymeric nanoparticles, and it can be positive for fabricating complex architectures, ranging from the micrometer to centimeter in scale (Fig. 8B). Although its use for fabricating micro- and nanomotors is severely restricted, it can be useful when combined with other techniques in order to create more complex structures [142,151,152].

2.3. Electroless deposition

Electroless deposition is an electrochemical deposition process in which a reducing agent dissolved in media provides the electrons, meaning that no external power is involved. The formula in Equation 2 represents the process [153–156]:

$$M^{n+}_{(aq)} + Red_{(aq)} \rightarrow M_{(s)} + Ox_{(aq)} \quad (2)$$

In electroless deposition, the driving force behind the reduction of metal ions and their deposition is provided by a chemical-reducing agent in solution that delivers its electrons via a catalytic surface. In that autocatalytic process, the metal catalyzes its own subsequent deposition. Electroless deposits of Ni, Co, Sn, Rh, Ru, Pd, Pt, Cu, Au and Ag metals can be easily obtained; however, others are possible if co-deposited with Ni [150,156]. Not to be confused with the galvanic displacement reaction, which does not require a reducing agent in the electrochemical media, electroless deposition is applicable for the deposition of metals on irregularly shaped objects, holes, internal surfaces and non-conductive substrates, among others (Fig. 8C). As such, it is useful for synthesizing bio-hybrid micro- and nanomotors and for fabricating metallic core@shell micro-motors. The method can be also used to fabricate multi-segmented micro- and nanomotors; however, compared with electrodeposition, it affords considerably limited control [150,153,155,156].

3. Electrochemical characterization of micro- and nanomotors

Electrochemistry not only shows significant potential for synthesizing micro- and nanomotors but can also plays a considerable role in characterizing those new materials. Indeed, electrochemical analysis is pivotal in fabricating and characterizing materials, including micro- and nanomotors, such that separating their synthesis and characterization is often impractical.

Because electrochemical characterization requires micro- and nanomotors to make contact with a conductive or semiconductive surface, electrochemical techniques of characterization developed for bulk materials take advantage of their large surface areas relative to their mass, which increases their contact with surrounding materials and/or media. Nevertheless, the process requires sensitivity and selectivity as well as accuracy. Although all electrochemical techniques for characterizing micro- and nanomotors share several features, no single technique is superior, for they each depend on multiple factors that require rational consideration in relation to the material and application. Even so, the most popular are cyclic

voltammetry and electrochemical impedance spectroscopy [157–160]. Among their downsides, electrochemical techniques cannot offer information about an individual micro- or nanomotor. For that task, single-particle techniques can be used to isolate individual entities and identify their particular data, namely by significantly raising the number of measurements in order to statically confirm the response of a specific entity [158,160]. Electrochemical methods are very useful for characterizing micro/nanomotors; however, they must be coupled with optical and other methods for a holistic characterization of the system.

In what follows, common electrochemical techniques used for characterizing micro- and nanomotors are briefly discussed.

- **Potentiometry:** Potentiometric techniques allow measuring the potential of electrochemical cells under static conditions. To characterize nanomaterials, such techniques involve using various ion-selective electrodes to selectively convert the activity of a specific ion dissolved in solution into electrical potential. According to the Nernst equation, voltage depends upon the logarithm of ionic activity. Potentiometric techniques are especially useful for detecting and quantifying specific entities involved in corroding micro- and nanomotors, and scanning electrochemical microscopy in particular has been used to study such corrosion at the local level [157]. Potentiometric techniques also allow analyzing the chemical stability and surface properties of micro- and nanomotors, as well as their interaction with surrounding materials and/or media [158,160].
- **Voltammetry:** Voltammetric methods, including linear sweep voltammetry, cyclic voltammetry, polarography, and stripping voltammetry, are possibly the most important in electrochemical characterization and are widely used to quantitatively characterize inorganic and organic substances. In such methods, a controlled time-dependent potential is applied to a working electrode in an electrochemical cell and the resulting current measured. The time-dependent potential applied induces changes in the concentration of electroactive species on the electrode's surface due to their oxidation or reduction [159]. For example, differential pulse voltammetry (DPV) on a disposable screen-printed electrode was used to directly monitor the degradation of non-electroactive diphenyl phthalate into phenol in food and biological samples and to evaluate the degradation efficiency of Mg–Au Janus micromotors (Fig. 9A) [161]. As such research demonstrates, voltammetric methods are powerful electroanalytical techniques frequently used to monitor and analyze the efficiency of micro- and nanomotors for specific applications.

In the characterization of micro- and nanomotors, voltammetric techniques are especially useful in fundamental studies on oxidation and reduction processes in various media, adsorption processes on micro- and nanomotor surfaces, electron transfer and reaction mechanisms, and the kinetics of electron transfer processes. They can also be used to determine the effective surface area and chemical stability of nanomaterials, as well as their transport, chemical, speciation, and thermodynamic properties [158,160,162]. In the context of multicomponent or Janus micro- and nanomotors, the Tafel extrapolation of polarization curves has demonstrated excellence in determining the corrosion current density and, in turn, the corrosion rate. The approach is exceptionally useful for clarifying the mechanism of motility and the effect of external stimuli (e.g., light and ultrasound) and/or fuels (e.g., H_2O_2) on the mechanism of propulsion. The method requires the presence of a liner or Tafel section in the E versus log I curve. For bimetallic nanowires using H_2O_2 as fuel, all of which are based on the self-electrophoretic or bipolar electrochemical mechanism, it has been demonstrated that the speed is proportional to the mixed potential difference of the fuel at the corresponding metal segment [18]. As shown in Fig. 9B, the Tafel plots of Au, Pt, and Pt–CNT electrodes in a 5% wt. H_2O_2 solution revealed that the mixed potential of Au–Pt–CNT (i.e., ~72 mV) was significantly higher than Au–Pt (i.e., ~19 mV). That difference determined the strength of the locally generated electric field and the rate of electron transfer, which consequently determined the speed of the micromotors. Therefore, the incorporation of CNT into Pt segments has been shown to accelerate the propulsion of Au–Pt micromotors. Beyond that, the Tafel plots of anodic and cathodic H_2O_2 reactions or other fuels (e.g., glucose) allow predicting the direction of the motion of bimetallic micro- and nanomotors and facilitate the design of more versatile micro- and nanomotors [18,102,163].

- **Cyclic voltammetry**: In cyclic voltammetry, the current is registered by sweeping the potential back and forth between the chosen limits until the desired potential is reached, at which point the working electrode's potential drops in the opposite direction to return to the initial value. That cycle is usually repeated as many times as necessary. Cyclic voltammetry is extensively used in characterizing nanomaterials, especially their mechanisms and surface properties (e.g., effective surface area, reactivity, and stability, proper functionalization with (bio)molecules,…) [158,160,162,164]. Despite the multitude of applications for CV in the material characterization and evaluation of micro- and nanomotors regarding their efficiency in specific applications, evaluating processes of their surface modification and determining their electrochemical active surface areas (ECSA) are especially important tasks. As shown in Fig. 9C, electrochemical probes, including Fe(II)–Fe(III) voltammetric responses, are frequently used to evaluate the functionalization of micro- and nanomotor surfaces. Reducing such voltammetric responses is directly related to the accessible and active surface area and, in turn, allow detecting the surface's functionalization. Faradaic Fe(II)–Fe(III) processes are usually not completely obstructed, because the presence of organic molecules linked to the surface of micro- or nanomotors hinders but does not usually entirely block the mass transport of the Fe(II)–Fe(III) redox species. However, testing and, in some cases, quantifying the functionalization and coverage of the micro- or nanomotor's surface can be done efficiently [9,97]. On top of that, various CV-based approaches have been comprehensively examined to determine the ECSAs of various nanomaterials, including metallic micro- and nanomotors. The most widely used approach is hydrogen underpotential deposition (HUPD) on noble metals such as Pt, which involves using the hydrogen desorption charge from the CV to calculate ECSA values. Another well-established method is CO stripping, which involves using the charge associated with the oxidation of the previously adsorbed CO on the surface of micro- or nanomotors to determine ECSA values. For micro- and nanomotor-based materials that do not allow measuring HUPD (e.g., Au or Pd), ECSA values can be easily determined by using the charge associated with the reduction of the surface oxide. As shown in Fig. 9D, the micro- and nanomotors' surface was first oxidized by a potential sweep to yield an oxygen monolayer. In a subsequent cathodic sweep, the charge needed to reduce the oxide layer was integrated and used to determine ECSA values [9,165].
- **Polarography**: In polarography, a type of voltammetry, a dropping mercury electrode or static mercury drop electrode functions as a working electrode to offer a wide range of cathodic potential and a renewable surface. Polarographic techniques afford high accuracy and reproducibility, both of which are critical to characterizing nanomaterials, and are widely used for analytical purposes (e.g., determining numerous reducible species). [158,160].

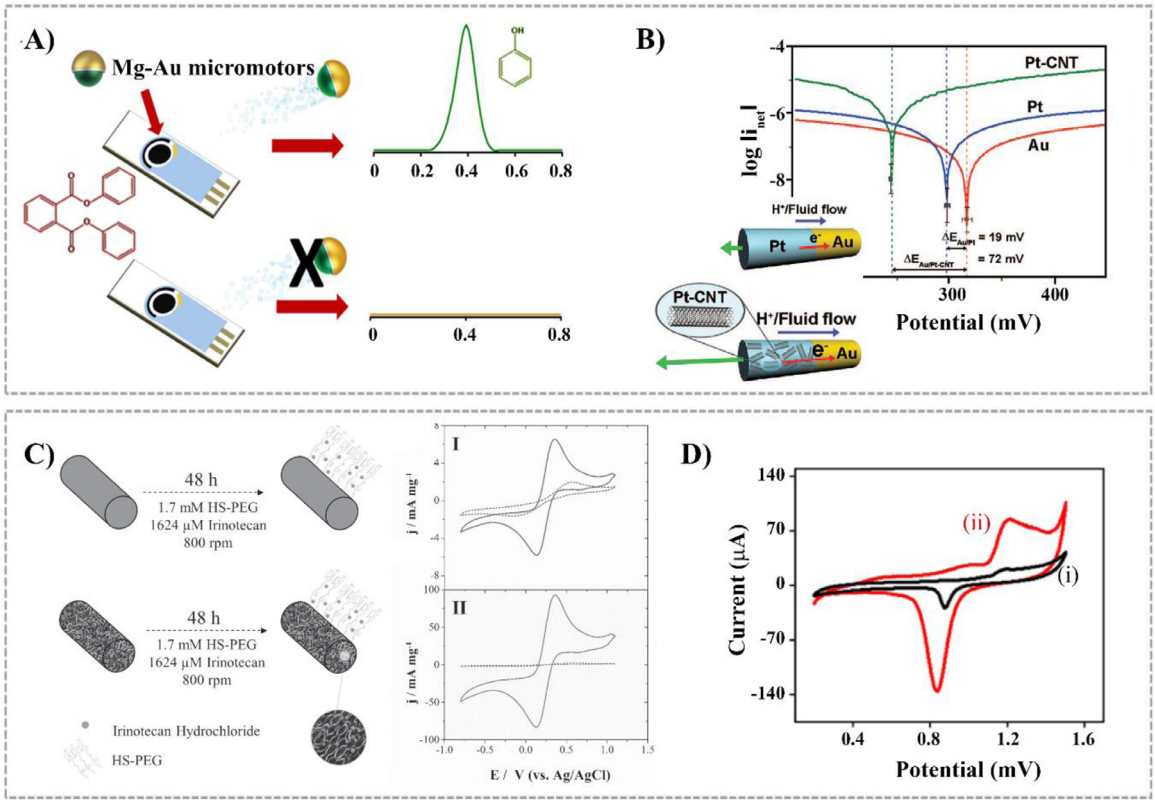

Fig. 9. (A) Schematic representation of Mg–Au Janus micromotor for the simultaneous degradation and detection of non-electroactive diphenyl phthalate into phenol. The differential pulse voltammetry signals of samples in the presence and absence of the Mg–Au Janus micromotor confirmed the degradation of diphenyl phthalate into phenol. Reproduced with permission from ref. [161]. Copyright 2016, American Chemical Society. (B) Tafel plots of Au, Pt, and Pt–CNT electrodes in a 5% wt. H_2O_2 solution. Differences in the mixed potentials are also indicated as ΔE. Reproduced with permission from ref. [101]. Copyright 2016, American Chemical Society. (C) Cyclic voltammograms of the Fe(II)–Fe(III) system in a KNO_3 0.2 M + $K_4[Fe(CN)_6]$ 2×10^{-3} M + $K_3[Fe(CN)_6]$ 2×10^{-3} M solution of compact and mesoporous CoNi@Au nanomotors before (continuous line) and after (dashed line) their functionalization with thiol-poly(ethylene glycol). Reproduced with permission from ref. [9]. Copyright 2016, Wiley. (D) Cyclic voltammograms of (i) nonporous and (ii) porous nanowires in H_2SO_4 0.1 M solution using a scan rate of 50 mV s^{-1}. Reproduced with permission from ref. [165]. Copyright 2016, American Chemical Society.

- **Electrochemical impedance spectroscopy**: A multifrequency AC electroanalytical method, electrochemical impedance spectroscopy measures the impedance of the electrode–solution interface over a wide range of frequencies, thereby allowing the determination of the polarization resistance (i.e., in the low-frequency region), the solution resistance (i.e., in the high-frequency region), and the capacitance of the double layer. Extremely useful for evaluating the electron-transfer properties of nanomaterials and understanding their chemical transformations, the method is often used to characterize nanomaterials, analyze their mechanistic and kinetic information, and study the corrosion, conductivity, semiconducting properties, chemical stability, and catalytic performance of micro- and nanomotors [158,160,162].
- **Zeta potential:** The zeta potential is the electric potential in the interfacial double layer of a dispersed entity (e.g., nanomaterial, micromaterial or droplets) versus a point of the mobile dispersion medium. It is a measure of the effective electric charge on the nanomaterial or micromaterial surface. The zeta potential is normally quantified by measuring the electrophoretic mobility of dispersed entities. The speed of entities in dispersed media is proportional to the field strength and their zeta potential. Therefore, entities (i.e., micro/nanomotors) that have a zeta potential will migrate toward an electrode if a field is applied. Zeta potential measurements are extremely useful [166–168] to characterize the electrophoretic mobility and surface charge of micro/nanomotors.

4. Applications

4.1. Biomedical applications

In recent years, researchers seeking to advance micro/nanomotors manufactured with electrochemical methods for use in biomedical applications have focused on integrating several functions as a means to fabricate truly multifunctional platforms. In the process, they initially prioritized the development of self-propelled machines based on the catalytic decomposition of various fuels, especially hydrogen peroxide, which generates oxygen bubbles that subsequently propel the motors [88,143,169–171]. One of the most popular mechanisms of propulsion to date is based on the catalytic decomposition of hydrogen peroxide using Pt-based micro/nanomotors. In the same early studies, researchers also focused on the effects of temperature, fuel concentration, micro/nanomotor shape and the composition of biological media with different degrees of ionic strength. In this sense, hard-template electrodeposition offers a powerful, inexpensive, reproducible technology for the mass synthetic production of nanowires, nanorods and tubular micro/nanomotors as well as helical, conical and other complex micromotors [25,88,100,143,172–175].

In the past decade, rigid single-component (e.g. Ni, Pt, Au, Fe and FePt) and multicomponent, multisegmented (e.g. Au–Pt, Ni–Pt and Cu–Pt) core@shell (e.g. Ni@Au and Fe@Au) and biohybrid (e.g. Au–Ni–yeast) nanowires and nanorods have been electrosynthesized using various types of hard-template electrodeposition [96,97,137]. To promote the biocompatibility of nanowires

and nanorods, posterior thermal treatment or a galvanic displacement reaction can be used to fabricate core@shell nanowires and nanorods. At the same time, surface functionalization can be used to promote their biocompatibility as well as reduce their agglomeration. Although asymmetry due to shape, structural imperfections or chemical composition along the nanowires and nanorods is pivotal for catalytic self-propulsion, the electrokinetic mechanism of the self-electrophoresis of the motion of nanowires, particularly multisegmented ones, in biological media or high-strength environments decreases their locomotion. Nanowires and nanorods also exhibit motion powered by ultrasound, electric, magnetic or acoustic fields, and in general, they are formed by rigid structures in contrast to biological systems. In order to mimic biological systems, especially to improve the locomotive mechanism of nanowires and nanorods, the synthesis of flexible, bi-segmented nanowires has been also investigated. Some flexible segmented nanowires containing joints of silver, gold or polymers can be obtained after the release of nanowire and nanorods by selective etching, with the replacement of sacrificial segments or by linking various nanowires using polymers [88,96,97,137,176].

Concentric mono- or bimetallic microtubes, also known as *micro-jets, nano-jets* or *tubular micro-engines*, based especially on Pt, facilitate the possibility of incorporating an inner catalytic surface for the decomposition of fuel and an external surface for further functionalization [143,172,173]. Therein, the mechanism of propulsion is similar to that of macroscopic jet engines. Conical, columnar or bi-conical microtubes, among ones with other shapes, can easily be synthesized by shape-controlled electrodeposition using anodic aluminum oxide or polymer templates, particularly cyclopore polycarbonate. Electrodeposition circumvents the more complex original pathway—that is, with rolled-up technology—based on the deposition of nanometer-thin layers that are ultimately rolled into tubular shapes [25,169,177–179]. In general, micro- and nano-jets are faster, minimize the concentration of hydrogen peroxide and afford a greater towing ability than nanowires and nanorods. In the past decade, the electrosynthesis of mono- and bimetallic concentric (e.g. Pt, Cu/Pt, Au/Pt), concentric metallic–polymeric (e.g. Pt/PANI, PEDOT–COOH–PEDOT/Ni/Pt) and bi-segmented (e.g. Au-Pt) or multisegmented (e.g. Au-Pt-Au) microtubes has been investigated [174]. In general, such efforts have focused on Pt-based micro-jets in order to understand and control the mechanism of self-propulsion using hydrogen peroxide, sometimes combined with an external stimulus (e.g. magnetic fields), and the effect of ionic strength and their locomotion in more complex media. Several researchers have also analyzed the functionalization, biocompatibility, internalization or cargo capabilities of drugs. However, using hydrogen peroxide as a fuel, even at very low concentrations, requires the use of Pt due to its superior catalytic efficiency compared to other materials that offer generally slow speeds, require high concentrations of chemical fuels and consequently demonstrate low potential for use in real biomedical applications [147,180–183]. During recent years, tubular, Pt-based (e.g. MoS_2/Pt) and Pt-free (e.g. Zn, PEDOT/MnO_2 and MoS_2/Au), self-propelled micromotors have been developed in order to minimize the fuel concentration and improve their biocompatibility, loading capacity and drug-delivery properties, among other features. In the process, their multiple functions for potential use in biomedical applications has been highlighted. Using Pt-free micromotors, however, can provide alternatives to hydrogen peroxide fuels, as exemplified by PANI/Zn microtubes that use acid as a fuel. In addition, the co-deposition of nanoparticles, whether magnetic or non-magnetic, as well as nanotubes and other nanostructures (e.g. SiO_2 NPs, Au NPs, Pt NPs, Fe_3O_4 NPs, carbon nanotubes, graphene quantum dots and polymeric NPs) during electrodeposition to create composite tubular micromotors (e.g. Zn-SiO_2 NPs, PEDOT/Pt NPs@CNT-PPy, reduced graphene oxide/Pt, reduced graphene oxide/Au, zirconia-graphene/Pt and graphene@Ag-MnO_2) has been revealed as an excellent strategy to tune the locomotive mechanism and improve their multifunctional properties [147,179–188]. More recently, researchers have devoted extraordinary efforts to develop multilayer tubular micromotors in order to incorporate an internal magnetic layer that can help to control the magnetic motion and external photocatalytic and electrocatalytic functional layers (e.g. Pt/Ni/WS_2 and Pt/Ni/Bi), all as a means to create more competitive multifunctional platforms [184]. For example, PPy-COOH/PPy/Ni/Pt tubular micromotors have been shown to be effective platforms for extracting nucleic acids [189]; Pt/Ni/Bi microtubes exhibit high heavy metal/DOX loading, a controllable release mechanism and excellent locomotion control [188]; and PEDOT/PtNPs@CNT-PPy micromotors can capture and destroy anthrax simulant spores [179]. Nevertheless, additional studies on the biocompatibility, stability and locomotion in real environments are greatly needed.

Helical micro/nanomotors, especially magnetic micro-helices, seem extremely promising for diverse *in vivo* applications, largely due to their locomotion performance. Helical nanomotors can be easily fabricated using the hard-template electrodeposition of Cu/Pd in aluminum oxide or polymeric templates followed by the selective etching of Cu, which can prompt the formation of Pd nano-helices with tunable lengths and diameters. Any Pd nanohelix can be covered with other metals or alloys by using electroless deposition [54,190]. Such a process allows the fabrication of hybrid nanomotors based on the connection of nanorod or nanowire segments with nano-helical segments that, by mimicking bacterial flagella, allow the fabrication of hybrid structures able to be displaced and controlled by means of magnetic or acoustic fields, if not both, without chemical fuels [61]. Beyond that, a micro-helix or more complex microstructures can be easily electrodeposited inside a photoresist template patterned by 3D laser lithography. Using 3D patterns for hybrid artificial bacterial flagella of CoNi-PPy or CoPt has been successful in electrodeposition and 3D laser lithography has allowed the electrosynthesis of multiple shapes [47,191,192]. However, additional studies are required to determine their potential for use in biomedical applications.

Electrochemical methods, especially electroless deposition, can also be easily combined with bio-templating and soft-template approaches to fabricate hybrid micro- or nanomotors. For example, magnetic CoNiReP helical structures have been synthesized by means of electroless deposition using lipids (i.e. helical liposomal microstructures). However, that strategy is more important for other possible applications, including environmental ones, than for biomedicine [193].

The emerging technology of micro/nanomotors offers enhanced opportunities to empower various biomedical applications, including disease diagnosis, targeted drug delivery, (bio-)sensing and noninvasive microsurgery, especially for the prevention and treatment of chronic diseases such cancer, due to their autonomous propulsion and integrated versatile functions. In that light, artificial micro/nanomotors should satisfy certain prerequisites for real *in vivo* biomedical applications, including biocompatibility or biodegradability, if not both, and precise real-time control of micro/nanomotor dynamics (i.e. spatiotemporal resolution at the whole-body scale). The driving force to control the micro/nanomotor movement could be given by external stimuli such as magnetic, electric, ultrasound, light irradiation or sensing *in situ* gradients such as pH, temperature or chemical composition (i.e., chemical fuels), ideally available in biological fluids. Another prerequisite is high cargo-loading capabilities and controlled drug release, especially for targeted drug delivery applications. Current artificial micro/nanomotors synthesized using electrochemical deposition (e.g. electrodeposition, electrophoretic deposition and electroless deposition) tested for biomedical applications consist

of single- or multicomponent micro/nanostructures with different shapes and architectures as well as based on magnetic materials, alloys, noble metals, semiconductors or conductive polymers. Electrodeposited materials can be easily integrated into microorganisms, or else several metals can be directly grown on microorganisms by using electroless deposition, to induce the formation of bio-hybrid micro/nanomotors.

4.2. Environmental applications

The second major potential application of micro and nanomotors is in the environmental field. Micro and nanomotors show some advantages – continuous motion, force, high surface area, functionality- that are making them very promising to fight against the environmental pollution associated to the increasing anthropogenic/human activities and causing non-negligible issues all over the world. The micromotors have found interest not only in adsorption and/or degradation of chemical pollutants and pathogenic microorganisms (bacteria) but also in environmental sensing and monitoring. Electrochemistry has played a fundamental role in the fabrication of micromotors for the already mentioned tasks as it will be detailed below. One important issue that the authors would like to highlight and in line with what stated before is that nanomotors must be designed keeping in mind the targeted pollutant and the mode of propulsion. The former aspects will define not only the kind of functional materials to be used but also the shape of the micromotors.

Two different strategies have been followed for water decontamination. The first one consists on the adsorption of the pollutants onto the microswimmers. Meanwhile the second one is based on the catalytic degradation of the pollutant on the motor surface. The first reported micromotor on pollutant removal was done by the group of Prof. Wang (Fig. 10) [194]. This group prepared a self-propelled Au/Ni/PEDOT/PT multilayered tubular micromotor prepared by template-assisted electrodeposition using a polycarbonate membrane. Once released from the membrane, the microrobots were further modified with long-chain self-assembled alkanethiol monolayers (SAM) conferring high hydrophobicity to the outer gold layer. While the SAM monolayer allowed the interaction with the oil droplets and therefore their collection and removal from water, the inner Pt layer catalytically decomposed the chemical fuel (H_2O_2) into oxygen bubbles creating the propulsion forces needed to move them. Other electrodeposited micromotors exploiting the strategy of removal of pollutants have been developed by Pumera's group using DNA-functionalized Au/Pt microtubes. First, Au/Pt microtubes were fabricated again by template-assisted electrodeposition. After that, DNA was anchored onto the outer gold layer as it has high adsorption capability for the toxic Hg(II) ions due to the high specificity and strong binding of Hg(II) toward the T-T mismatched pairs in DNA [195]. Or the group of Prof. Sánchez who developed graphene oxide/Ni/Pt tubular microrobots for the removal of toxic heavy metals like lead [196]. Each material provided with a different functionality: While graphene oxide is responsible for lead capture, nickel layer confers external magnetic control and Pt is the engine decomposing H_2O_2 fuel into O_2 for self-propulsion. The authors demonstrated a higher efficiency removal of lead compared to nonmotile swimmers. A very important aspect is that these structures can be regenerated to reuse them. Many other developments have been successful to recover other chemical pollutants apart from heavy metals and oil from contaminated water. For example, Virendra et al. fabricated multi-layered self-propelled ZrO_2/Graphene oxide/Pt conical microtube for the selective capture of nerve agents [181]. These micromotors were synthesized by template electrochemical method in a two-step process. First, zirconia and graphene oxide were simultaneously deposited. The surface properties of graphene make it an excellent template for the synthesis of high-surface area ZrO_2 nanostructures, which at the end is the responsible of the selective binding and recovery of organophosphate compounds. After that, a Pt inner layer was electrodeposited to get self-propelled swimmers using H_2O_2 as fuel. The properties of graphene also allow obtaining a highly porous Pt layer favoring high micromotor' speeds. These structures have been successful in removing different nerve agents like methylparoxon, ethylparoxon or bis-4-paraphenol. Finally, they have also demonstrated that the micromotors can be regenerated and the nerve agents recovered by alkali treatment, making the whole process more economically viable. Or Uygun et al. prepared COOH-PPy:PEDOT/Pt tubular micromotors functionalized with carbonic anhydrase (CA), a zinc metalloenzyme that catalyzes the hydration of CO_2 to bicarbonate and further mineralized to $CaCO_3$ [197]. The micromotors are self-propelled due to the presence of Pt inner layer and H_2O_2 fuel. This study shows how these micromotors can sequestrate CO_2 in an efficient and rapid manner. The continuous motion of the CA-functionalized structures accelerates the biocatalytic activity of the enzyme because the enhanced fluid transport and therefore diffusion. Thus, functionalized micro/nanotubes can rapidly adsorb and collect toxic chemicals (heavy metals, oil, CO_2,…) while moving in solution, making it a promising methodology to decontaminate water.

The second strategy also widely investigated is the degradation of pollutants employing advanced oxidation processes able to remove either organic or inorganic pollutants using oxidants like hydroxyl radicals, hydrogen peroxide or ozone and/or UV-light to catalyze the reactions. One of the first works was done by Orozco et al. who reported the electrodeposition of PEDOT/Fe microtubular motors for the detoxification of chemical warfare agents like organophosphorus nerve agents [198]. The micromotors were placed in a solution containing the nerve agent as well as hydrogen peroxide (it was added with a dual role: oxidation agent and micromotor's fuel), $NaHCO_3$ or NaOH (as peroxide (OOH^-) activator) and the surfactant sodium cholate (to improve bubble formation). The authors observed that the *in situ* generation of OOH^- nucleophiles under the presence of the micromotors favored the oxidation of the organophosphate agent into *p*-nitrophenol under quiescent conditions and with a high yield. They attributed such good decontamination results to the enhanced convection and mass transport induced by the motion of the micromotors. Later, Garcia-Torres et al. make use of the catalytic properties of the outer Pt shell in mesoporous CoNi@Pt rods to enhance the oxidation of azo dyes by sodium borohydride ($NaBH_4$) (Fig. 10). They prepared the mesoporous nanorods by using a double template: a hard template to confer the cylindrical shape and then a soft template to create the mesoporosity. The high mesoporosity obtained was crucial to have a high surface area and therefore a big enhancement in the efficiency of oxidation, making the degradation faster. On the other hand, they propelled the micromotors using a magnetic field due to the CoNi core. This magnetic maneuverability allowed controlling the directionality of pollutants degradation. Moreover, they were easily recovered and recycled due to their magnetic character [199].

Photocatalytic micro/nanomotors have been also fabricated using electrodeposition due to their promising applicability in water remediation. The irradiation of a semiconductor generates electron-hole pairs that in turn induces oxidation-reduction reactions. While the electrons react with the oxygen present to give superoxide radicals and hydrogen peroxide, the holes interact with water or OH^- groups to generate hydroxyl radicals. All these highly reactive oxidants are responsible for the degradation of the pollutants. For example, Pané and collaborators developed new hybrid micromotors consisting on a magnetic CoNi segment and a photocatalytic Bi_2O_3/BiOCl segment by a two-step electrodeposition process. They conferred different shapes to the micromotors -cylinders

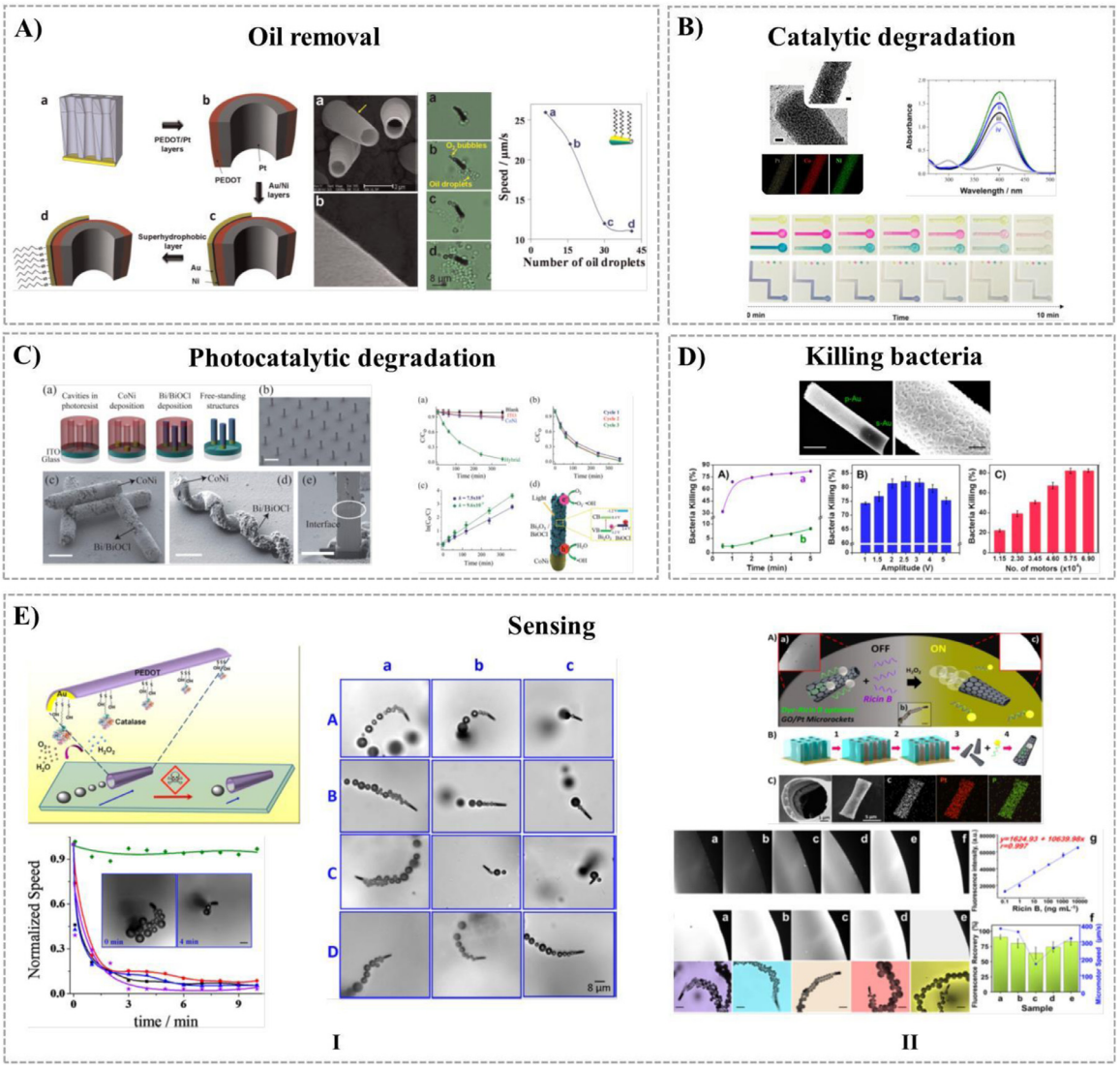

Fig. 10. (A) Schematic procedure for the synthesis of micromotors. First, a PEDOT/Pt bilaye microtube is electrochemically deposited followed by vapor deposition of Ni and Au layer. Finally, the outer rough Au layer was functionalized with a self-assembled alkanethiol monolayer for an effective interaction and capture of oil droplets. Reproduced with permission from refence [194]. Copyright 2012, American Chemical Society. (B) SEM and EDX images of mesoporous CoNi@Pt core-shell nanorods. The Pt shell catalyzes the degradation reaction and the CoNi core allows magnetic control of the degradation path. Reproduced with permission from refence [199]. Copyright 2017, American Chemical Society. (C) Scheme for the fabrication of CoNi-Bi_2O_3/BiOCl bisegmented nanorods and nanohelices for photocatalytic remediation of contaminated water and with magnetic control. Reproduced with permission from refence [200]. Copyright 2015, Royal Society of Chemistry. (D) Lysozyme-modified Au nanorods propelled through acoustic waves for bacteria killing. The efficiency depends on the time and amplitude of ultrasounds treatment and the amount of nanomotors. Reproduced with permission of refence [165]. Copyright 2015, American Chemical Society. (E) (I) PEDOT/Au microcones functionalized with catalase for the biocatalytic propulsion of the micromotor and use for water quality testing based on changes in the motion characteristics under the presence of pollutants. The graph and the images show changes in the swimming behavior upon exposure to different pollutants (Hg, Cu, sodium azide and aminotrizole). Reproduces with permission from refence [204]. Copyright 2012, American Chemical Society. (II) Synthesis scheme, SEM and EDX images of a reduced graphene oxide (rGO)/platinum micromotor modified with an aptamer tagged with a dye for the fluorescent detection of ricin B toxin. Graphs showing the fluorescence recovery due to the binging of the ricin to the aptamer as a function of incubation time and H_2O_2 concentration. Fluorescent images and optical images of the micromotor at different fuel levels. Reproduced with permission from refence [207]. Copyright American 2016, Chemical Society.

and helices- using membranes obtained by 3D photolithography. The CoNi segments allowed magnetic control of the micromotors and easy recovery after treatment for reuse. Meanwhile, the UV-light irradiation of the photocatalytic Bi_2O_3/BiOCl segment induced the oxidation of rhodamine blue (RhB) with a 90% efficiency and within 6h [200]. The same group has also reported the electrochemical synthesis of coaxial TiO_2-PtPd-Ni tubular structures for the photocatalytic purification of contaminated water using anodized aluminum oxide (AAO) membranes. During the synthesis, a thermal treatment was required to obtain the TiO_2 layer. The coaxial nanotubes were able to degrade 100% of dyes (Rhodamine Blue, methyl orange and methylene blue) in just 30 min under sunlight [201].

On the other hand, these tiny nanostructures have also been employed to kill pathogenic microorganism that can be found in contaminated waters. Thus, some functionalized microswimmers have been successfully proved to kill microbial pathogens. Fig. 10 illustrates porous Au nanowires functionalized with lysozyme, an antibacterial agent. The porous nanowires have been prepared by electrodeposition using AAO membrane as a template. An Au-Ag allow was electroplated inside the pores of the membrane followed by dealloying silver using a 35% HNO_3 solution to confer the porosity. The mechanism of action of the enzyme is based on the cleavage of the glycosidic bonds of the peptidoglycans present in the bacteria cell walls. This enzyme has been studied alone as an antibacterial agent or encapsulated into different solid

materials like capsules or polymers to increase the enzyme's stability and reusability. But the limitation of this strategy is the accumulation of the dead bacteria onto the surface of the composites hindering the efficiency of the enzyme. This limitation is overcome by the ultrasound propulsion of the lysozyme-loaded nanomotors offering an efficient and fast destruction of different types of bacteria like gram-positive *Micrococcus lysodeikticus* and Gram-negative *Escherichia coli*. The motion of the swimmers impacts on their performance as the fluid mixing not only favors the enzyme-bacteria interaction but also avoids accumulation of the death bacteria onto their surface. These advantages lead a 30-fold increase in bacteria destruction efficiency compared to the static nanomotors. Moreover, the high porosity of the gold segment also impacts on the efficiency as a higher amount of lysozyme can be loaded into the micromotors [165]. Or Orozco et al. prepared multi-layered microtubes comprising an outer layer of PPy and PEDOT, an intermediate magnetic Ni layer and an inner catalytic Pt layer. These micromotors were prepared by a three-step electrodeposition process using polycarbonate membrane as a template. After their release from the membrane, the outer layer was further functionalized with the *Bacillus globilli* antibody to recognize and trap innocuous *Bacillus globigii* spores used to simulate the dangerous anthracis spores. On the other hand, the Ni layer served for magnetic guidance and the Pt layer to decompose H_2O_2 and promote self-propulsion. Moreover, H_2O_2 also was used as antimicrobial agent to degrade the cells. Thus, the mixture of the micromotors and the antibacterial agent led to an increase in the number of damaged cells. Such increase was not detected without micromotors [179].

Finally, micromotors have been also developed to display other functionalities like sensing and monitoring, which are essential tasks for water remediation. Different types of electrodeposited micro/nanomotors have been fabricated to up to day to sense a wide variety of pollutants like heavy metal ions, organic molecules and pathogenic bacteria. Moreover, different strategies have been studied to sense such variety of chemicals all attributed to the presence of the analyte: (i) changes in the micromotor's swimming behavior (e.g. speed, movement), (ii) changes in the fluorescence or (iii) chemical reaction occurring on the micromotor's surface. The group of Prof. Wang was the first reporting micromotors able to sense metallic ions based on their motion. They developed Au-Pt bisegmented nanowires by electrodeposition able to correlate the micromotor speed with the concentration of silver ions (Ag(I)), the analyte, keeping the fuel (H_2O_2) concentration constant. The reduction of Ag(I) onto the micromotor improved its catalytic performance and therefore increased its speed [202]. However, the opposite can also occur since the presence of other metallic ions poisons the catalyst leading to a lower speed. For example, electrochemically synthesized Cu/Pt microtubes decreases their velocity under the presence of Pb^{2+} which was higher as the ions concentration increased up to a given concentration [203]. A similar strategy consisted on attaching enzymes onto the micromotor surface and the inhibition of the enzyme by the analyte/s reduces the microswimmer velocity. For example, catalase-based PEDOT/Au tubular micromotors reduced their speed under the presence of contaminants like Hg(II) or Cu(II). They inhibited the activity of the enzyme -powering the microstructures by transforming H_2O_2 into O_2 and H_2O- and therefore the swimming performance [204]. Enzyme-based micromotors have also been developed for sensing organic molecules like the work of Singh et al. who developed catalase-functionalized PEDOT/Au microtubes for the sensing of nerve agents vapor plumes. They observed a decrease in the micromotor speed due to the inhibition of the enzyme [205].

The second sensing strategy is based on the quenching of fluorescence micromotors by some contaminants. For example, Beatriz Jurado and coworkers fabricated tubular PEDOT/Pt micromotors by electrodeposition and further modified them first with polystyrene sulfonate (PSS) and poly(diallyldimethylammonium chloride) (PDDA) and then with CdTe quantum dots. Mercury ions (Hg^{2+}) adsorbed onto the QD's causing the reduction in the fluorescence emission. Moreover, this sensor allowed the discrimination between Hg^{2+} and other mercury species (e.g. CH_3Hg^+) and coexisting ions (e.g. Pb^{2+}) [206]. More recently, micromotors have been functionalized with selective molecules to confer specificity towards a given analyte. For example, aptamers -single DNA strands- have been attached to micromotors surface to recognize and capture target molecules. Esteban-Fernández de Ávila et al. have fabricated micromotors based on reduced graphene-oxide (rGO) and platinum for the detection of ricin. The micromotor was modified with a ricin B aptamer tagged with a fluorescent dye to confer specificity towards ricin. The aptamers are stuck onto the carbon surface trough p-p interaction between carbon and nucleotide bases of DNA. In this situation, the fluorescence of the dye is quenched. However, when ricin B is attached to the aptamer-dye conjugate fluorescence is restored. The fluorescence emission was highly enhanced when the micromotors were propelled in the solution indicating a better interaction between the toxin and the micropropellers. Moreover, they also reported the specific interaction between ricin and the micromotors under the presence of other proteins or toxins as interferents (Fig. 10) [207]. Similar reported works used graphene/Pt or graphene/Ni/Pt microtubes functionalized with fluorescent-labelled aptamers for the detection of fumonosin B1 and ochratoxin A, mycotoxins found in food samples [208,209]. To summarize, it is evident that the field of micro and nanorobotics offers considerable promise for addressing growing challenges not only in the biomedical field but also for environmental applications. The functionality and the size are attractive characteristics for them to show high performance applications.

5. Conclusion and outlook

Artificial micro- and nanomotors have emerged as a technology in demand to perform complex tasks at the nanoscale. Although the full applicability of artificial micro- and nanomotors remains far from realized, several important achievements toward reaching that goal have been made in the past 15 years. This progress report provides an overview of general developments in the materials and shapes of artificial micro- and nanomotors, techniques used in their fabrication, their surface functionalization, and the mechanisms of their modification, propulsion, actuation, and navigation. Beyond that, it reviews the outstanding merits of electrochemically manufactured artificial micro- and nanomotors in certain potential applications, including ones in biomedicine and environmental remediation, which require controlling locomotion in complex environments mimicking biological media or wastewater.

Although techniques to effectively control their mechanisms of mobility remain underdeveloped, impressive advances in both externally driven (e.g., light, ultrasound, magnetic, and electrical) and fueled artificial nano- and micromotors with a capacity for self-propulsion have been made in recent years. Despite the importance of those mechanisms, the nature and shape of micromotors essentially determines not only their properties and applicability but also which techniques may be used to fabricate them. For that reason, the manufacture of the devices also warrants consideration, because their application and universalization, despite the excellent properties that they may possess, lies in the cost of production, which is largely determined by the costs of the base materials and their fabrication. In that sense, the relative simplicity and low cost of the equipment and manufacturing process, as well as their potential scalability for industrial production, make electrochemical deposition a valuable tool for the mass fabrication of artificial micro- and nanomotors. Electrochemical methods are also positioned as powerful techniques not only for the fabrication

of microrobots but also for their characterization and even propulsion. However, on both fronts, several challenges remain to be addressed. Herein, we overview the potential use of electrochemistry to fabricate and characterize microrobots as well as the state of the art of electrosynthesized micro- and nanomotors.

The principal challenges of electrochemically engineering micro- and nanomotors to meet the exact needs of target applications relate to the need to precisely control their shape, size, and material composition. However, by capitalizing upon template-assisted manufacturing, including methods of electrodeposition, the batch production of well-defined, multicompositional architectures can be achieved. Even then, the production of such structures requires robust knowledge about not only synthesis and manufacturing but also about engineering, particularly to expand fabrication processes to the industrial scale. Beyond that, several risks and obstacles associated with their production have been identified, including the incompatibility of certain materials with the fabrication sequence, suboptimal adhesion between components, and the complexity of précising controlling the shape, size, and material composition during upscaling. For one, even though electrochemical methods, especially cyclic voltammetry, can provide useful information about micro- and nanomotors, a facile, rapid, reliable, and efficient method of characterizing them, if not nanomaterials in general, remains to be developed to optimize the fabrication process. For another, electrochemical techniques, though especially efficient in analyzing the electrical and chemical properties (e.g., composition, surface chemistry, stability, and reactivity) of nanomaterials, need enhanced sensitivity, accuracy, and selectivity to improve the design of micro- and nanomotors.

While advances in electrochemical techniques of characterization stand to expand the applicability of nanomaterials once characterized, applications of micro- and nanomotors in biomedicine and environmental remediation remain only in the proof-of-concept stage. Gauging their potential impact, especially their applicability in biomedicine, requires understanding and, in turn, controlling their performance in complex, real-world environments. Concerning biomedical applications in particular, both *in vitro* and *in vivo* animal tests have demonstrated the promise of self-propelled and externally driven micro- and nanomotors for use in novel nanomedical platforms. Moreover, for drug delivery platforms, micro- and nanomotors may also integrate high cargo-loading capabilities and controlled drug release. Despite such advances, challenges remain in holistically meeting requirements for the biocompatibility, biodegradability, and precise, real-time control of micro- and nanomotor dynamics in complex biological fluids. Innovations in forms of administration are also strongly encouraged, including ones that can take advantage of surface functionalization, which has been characterized as a powerful tool for tuning and improving the navigation, penetration, retention, and cell manipulation of micro- and nanomotors. In short, although micro- and nanomotors are far from ready for clinical use, they will enter into extended universal practice in the near future.

In environmental applications, micro- and nanomotors have been hailed as excellent platforms for water toxicity screening and accelerated remediation processes via the adsorption of heavy metals and/or organic pollutants, if not also the latter's degradation and/or mineralization. They can also play an important role in inhibiting bacterial growth or killing bacteria and other harmful micro-organisms, as well as can be especially useful in inaccessible environments. Nevertheless, their realistic applicability in environmental remediation and pollutant monitoring requires controlling their locomotion in complex environmental media (e.g., wastewater), improving their reusability and recyclability, and ensuring their biodegradability or at least easy recuperation, following their identification as a new pollutant in aquatic media, one demonstrating significant toxicity and other negative effects in relation to aquatic biota. Added to that, upscaling the production of micro- and nanomotors requires a cost-effective means of fabricating them or at least the possibility of monitoring and/or remediating large contaminated areas and large volumes of wastewater. Even confronted with those challenges, the use of micromotors in large-scale environmental applications is expected to be widespread in the not-so-distant future.

Declaration of Competing Interest

The authors declare that they have no known competing financial interests or personal relationships that could have appeared to influence the work reported in this paper.

Acknowledgements

A.S. would like to acknowledge funding from the EMPAPOSTDOCS-II program. The EMPAPOSTDOCS-II program has received funding from the European Union's Horizon 2020 research and innovation program under the Marie Skłodowska-Curie grant agreement number 754364. J.G.-T. acknowledges the Serra Hunter program of the *Generalitat de Catalunya*.

References

[1] M. Sitti, Miniature soft robots - road to the clinic, Nat. Rev. Mater. 3 (2018) 74–75, doi:10.1038/s41578-018-0001-3.
[2] B.J. Nelson, I.K. Kaliakatsos, J.J. Abbott, Microrobots for minimally invasive medicine, Annu. Rev. Biomed. Eng. 12 (2010) 55–85, doi:10.1146/annurev-bioeng-010510-103409.
[3] W. Hu, G.Z. Lum, M. Mastrangeli, M. Sitti, Small-scale soft-bodied robot with multimodal locomotion, Nature 554 (2018) 81–85, doi:10.1038/nature25443.
[4] P. Fischer, A. Ghosh, Magnetically actuated propulsion at low Reynolds numbers: towards nanoscale control, Nanoscale 3 (2011) 557–563, doi:10.1039/c0nr00566e.
[5] A. Credi, Nanomachines. Fundamentals and applications. By Joseph Wang., Angew. Chemie Int. Ed 53 (2014) 4274–4275, doi:10.1002/anie.201311274.
[6] G. Zhao, A. Ambrosi, M. Pumera, Self-propelled nanojets via template electrodeposition, Nanoscale 5 (2013) 1319–1324, doi:10.1039/c2nr31566a.
[7] S. Tottori, L. Zhang, F. Qiu, K.K. Krawczyk, A. Franco-Obregõn, B.J. Nelson, Magnetic helical micromachines: fabrication, controlled swimming, and cargo transport, Adv. Mater. 24 (2012) 811–816, doi:10.1002/adma.201103818.
[8] M. Fernández-Medina, M.A. Ramos-Docampo, O. Hovorka, V. Salgueiriño, B. Städler, Recent advances in nano- and micromotors, Adv. Funct. Mater. 30 (2020) 1–17, doi:10.1002/adfm.201908283.
[9] A. Serrà, N. Gimeno, E. Gómez, M. Mora, M.L. Sagristá, E. Vallés, Magnetic mesoporous nanocarriers for drug delivery with improved therapeutic efficacy, Adv. Funct. Mater. 26 (2016) 6601–6611, doi:10.1002/adfm.201601473.
[10] C. Zhou, L. Zhao, M. Wei, W. Wang, Twists and turns of orbiting and spinning metallic microparticles powered by megahertz ultrasound, ACS Nano 11 (2017) 12668–12676, doi:10.1021/acsnano.7b07183.
[11] D. Schamel, A.G. Mark, J.G. Gibbs, C. Miksch, K.I. Morozov, A.M. Leshansky, P. Fischer, Nanopropellers and their actuation in complex viscoelastic media, ACS Nano 8 (2014) 8794–8801, doi:10.1021/nn502360t.
[12] S. Pané, J. Puigmartí-Luis, C. Bergeles, X.Z. Chen, E. Pellicer, J. Sort, V. Počepcová, A. Ferreira, B.J. Nelson, Imaging technologies for biomedical micro- and nanoswimmers, Adv. Mater. Technol. 4 (2019) 1–16, doi:10.1002/admt.201800575.
[13] G.T. van Moolenbroek, T. Patiño, J. Llop, S. Sánchez, Engineering intelligent nanosystems for enhanced medical imaging, Adv. Intell. Syst. 2000087 (2020) 2000087, doi:10.1002/aisy.202000087.
[14] J. Vyskočil, C.C. Mayorga-Martinez, E. Jablonská, F. Novotný, T. Ruml, M. Pumera, Cancer cells microsurgery via asymmetric bent surface Au/Ag/Ni microrobotic scalpels through a transversal rotating magnetic field, ACS Nano 14 (2020) 8247–8256, doi:10.1021/acsnano.0c01705.
[15] K. Villa, J. Vyskočil, Y. Ying, J. Zelenka, M. Pumera, Microrobots in brewery: dual magnetic/light-powered hybrid microrobots for preventing microbial contamination in beer, Chem. - A Eur. J. 26 (2020) 3039–3043, doi:10.1002/chem.202000162.
[16] S. Fournier-Bidoz, A.C. Arsenault, I. Manners, G.A. Ozin, Synthetic self-propelled nanorotors, Chem. Commun. (2005) 441–443, doi:10.1039/b414896g.
[17] W.F. Paxton, K.C. Kistler, C.C. Olmeda, A. Sen, S.K. St. Angelo, Y. Cao, T.E. Mallouk, P.E. Lammert, V.H. Crespi, Catalytic nanomotors: autonomous movement of striped nanorods, J. Am. Chem. Soc. 126 (2004) 13424–13431, doi:10.1021/ja047697z.
[18] Y. Wang, R.M. Hernandez, D.J. Bartlett, J.M. Bingham, T.R. Kline, A. Sen, T.E. Mallouk, Bipolar electrochemical mechanism for the propulsion of catalytic nanomotors in hydrogen peroxide solutions, Langmuir 22 (2006) 10451–10456, doi:10.1021/la0615950.

[19] P.M. Wheat, N.A. Marine, J.L. Moran, J.D. Posner, Rapid fabrication of bimetallic spherical motors, Langmuir 26 (2010) 13052–13055, doi:10.1021/la102218w.
[20] T.C. Lee, M. Alarcón-Correa, C. Miksch, K. Hahn, J.G. Gibbs, P. Fischer, Self-propelling nanomotors in the presence of strong Brownian forces, Nano Lett 14 (2014) 2407–2412, doi:10.1021/nl500068n.
[21] K.M. Manesh, M. Cardona, R. Yuan, M. Clark, D. Kagan, S. Balasubramanian, J. Wang, Template-assisted fabrication of salt-independent catalytic tubular microengines, ACS Nano 4 (2010) 1799–1804, doi:10.1021/nn1000468.
[22] A.A. Solovev, Y. Mei, E.B. Ureña, G. Huang, O.G. Schmidt, Catalytic microtubular jet engines self-propelled by accumulated gas bubbles, Small 5 (2009) 1688–1692, doi:10.1002/smll.200900021.
[23] R. Liu, A. Sen, Autonomous nanomotor based on copper-platinum segmented nanobattery, J. Am. Chem. Soc. 133 (2011) 20064–20067, doi:10.1021/ja2082735.
[24] R.F. Ismagilov, A. Schwartz, N. Bowden, G.M. Whitesides, Autonomous movement and self-assembly, Angew. Chemie - Int. Ed. 41 (2002) 652–654, doi:10.1002/1521-3773(20020215)41:4⟨652::AID-ANIE652⟩3.0.CO;2-U.
[25] W. Gao, S. Sattayasamitsathit, J. Orozco, J. Wang, Highly efficient catalytic microengines: Template electrosynthesis of polyaniline/platinum microtubes, J. Am. Chem. Soc. 133 (2011) 11862–11864, doi:10.1021/ja203773g.
[26] J.G. Gibbs, Y.P. Zhao, Autonomously motile catalytic nanomotors by bubble propulsion, Appl. Phys. Lett. 94 (2009) 3–6, doi:10.1063/1.3122346.
[27] M. Xuan, Z. Wu, J. Shao, L. Dai, T. Si, Q. He, Near infrared light-powered janus mesoporous silica nanoparticle motors, J. Am. Chem. Soc. 138 (2016) 6492–6497, doi:10.1021/jacs.6b00902.
[28] Y. Mei, A.A. Solovev, S. Sanchez, O.G. Schmidt, Rolled-up nanotech on polymers: from basic perception to self-propelled catalytic microengines, Chem. Soc. Rev. 40 (2011) 2109–2119, doi:10.1039/c0cs00078g.
[29] W. Gao, A. Pei, X. Feng, C. Hennessy, J. Wang, Organized self-assembly of janus micromotors with hydrophobic hemispheres, J. Am. Chem. Soc. 135 (2013) 998–1001, doi:10.1021/ja311455k.
[30] J. Zhang, S. Agramunt-Puig, N. Del-Valle, C. Navau, M.D. Baró, S. Estradé, F. Peiró, S. Pané, B.J. Nelson, A. Sanchez, J. Nogués, E. Pellicer, Tailoring staircase-like hysteresis loops in electrodeposited trisegmented magnetic nanowires: a strategy toward minimization of interwire interactions, ACS Appl. Mater. Interfaces. 8 (2016) 4109–4117, doi:10.1021/acsami.5b11747.
[31] T.Y. Huang, M.S. Sakar, A. Mao, A.J. Petruska, F. Qiu, X.B. Chen, S. Kennedy, D. Mooney, B.J. Nelson, 3D printed microtransporters: compound micromachines for spatiotemporally controlled delivery of therapeutic agents, Adv. Mater. 27 (2015) 6644–6650, doi:10.1002/adma.201503095.
[32] L. Zhang, J.J. Abbott, L. Dong, B.E. Kratochvil, D. Bell, B.J. Nelson, Artificial bacterial flagella: fabrication and magnetic control, Appl. Phys. Lett. 94 (2009) 2007–2010, doi:10.1063/1.3079655.
[33] U. Bozuyuk, O. Yasa, I.C. Yasa, H. Ceylan, S. Kizilel, M. Sitti, Light-triggered drug release from 3d-printed magnetic chitosan microswimmers, ACS Nano 12 (2018) 9617–9625, doi:10.1021/acsnano.8b05997.
[34] M.T. Bryan, J. Garcia-Torres, E.L. Martin, J.K. Hamilton, C. Calero, P.G. Petrov, C.P. Winlove, I. Pagonabarraga, P. Tierno, F. Sagués, F.Y. Ogrin, Microscale magneto-elastic composite swimmers at the air-water and water-solid interfaces under a uniaxial field, Phys. Rev. Appl. 11 (2019) 1–12, doi:10.1103/PhysRevApplied.11.044019.
[35] P. Calvo-Marzal, S. Sattayasamitsathit, S. Balasubramanian, J.R. Windmiller, C. Dao, J. Wang, Propulsion of nanowire diodes, Chem. Commun. 46 (2010) 1623–1624, doi:10.1039/b925568k.
[36] K. Han, C.W. Shields, O.D. Velev, Engineering of Self-Propelling Microbots and Microdevices Powered by Magnetic and Electric Fields, Adv. Funct. Mater. 28 (2018) 1–14, doi:10.1002/adfm.201705953.
[37] R. Dong, Q. Zhang, W. Gao, A. Pei, B. Ren, Highly efficient light-driven TiO2-Au Janus Micromotors, ACS Nano 10 (2016) 839–844, doi:10.1021/acsnano.5b05940.
[38] L. Zhang, Z. Xiao, X. Chen, J. Chen, W. Wang, Confined 1d propulsion of metallodielectric janus micromotors on microelectrodes under alternating current electric fields, ACS Nano 13 (2019) 8842–8853, doi:10.1021/acsnano.9b02100.
[39] D.J. Peña, J.K.N. Mbindyo, A.J. Carado, T.E. Mallouk, C.D. Keating, B. Razavi, T.S. Mayer, Template growth of photoconductive metal-CdSe-metal nanowires, J. Phys. Chem. B. 106 (2002) 7458–7462, doi:10.1021/jp0256591.
[40] S. Ahmed, W. Wang, L. Bai, D.T. Gentekos, M. Hoyos, T.E. Mallouk, Density and shape effects in the acoustic propulsion of bimetallic nanorod motors, ACS Nano 10 (2016) 4763–4769, doi:10.1021/acsnano.6b01344.
[41] D. Ahmed, T. Baasch, B. Jang, S. Pane, J. Dual, B.J. Nelson, Artificial swimmers propelled by acoustically activated flagella, Nano Lett 16 (2016) 4968–4974, doi:10.1021/acs.nanolett.6b01601.
[42] M.M. Stanton, B.W. Park, A. Miguel-López, X. Ma, M. Sitti, S. Sánchez, Biohybrid microtube swimmers driven by single captured bacteria, Small 13 (2017) 1–10, doi:10.1002/smll.201603679.
[43] M.M. Stanton, J. Simmchen, X. Ma, A. Miguel-López, S. Sánchez, Biohybrid janus motors driven by escherichia coli, Adv. Mater. Interfaces. 3 (2016) 1–8, doi:10.1002/admi.201500505.
[44] X.Z. Chen, J.H. Liu, M. Dong, L. Müller, G. Chatzipirpiridis, C. Hu, A. Terzopoulou, H. Torlakcik, X. Wang, F. Mushtaq, J. Puigmartí-Luis, Q.D. Shen, B.J. Nelson, S. Pané, Magnetically driven piezoelectric soft microswimmers for neuron-like cell delivery and neuronal differentiation, Mater. Horizons. 6 (2019) 1512–1516, doi:10.1039/c9mh00279k.
[45] H.C.M. Sun, P. Liao, T. Wei, L. Zhang, D. Sun, Magnetically powered biodegradable microswimmers, Micromachines 11 (2020) 16–18, doi:10.3390/MI11040404.
[46] L. Schwarz, D.D. Karnaushenko, F. Hebenstreit, R. Naumann, O.G. Schmidt, M. Medina-Sánchez, A rotating spiral micromotor for noninvasive zygote transfer, Adv. Sci. 2000843 (2020) 1–14, doi:10.1002/advs.202000843.
[47] X.-Z. Chen, M. Hoop, F. Mushtaq, E. Siringil, C. Hu, B.J. Nelson, S. Pané, Recent developments in magnetically driven micro-and nanorobots, Appl. Mater. Today. 9 (2017) 37–48.
[48] P.J. Vach, P. Fratzl, S. Klumpp, D. Faivre, Fast magnetic micropropellers with random shapes, Nano Lett 15 (2015) 7064–7070, doi:10.1021/acs.nanolett.5b03131.
[49] S. Kim, S. Lee, J. Lee, B.J. Nelson, L. Zhang, H. Choi, Fabrication and manipulation of ciliary microrobots with non-reciprocal magnetic actuation, Sci. Rep. 6 (2016) 1–9, doi:10.1038/srep30713.
[50] T. Li, J. Li, H. Zhang, X. Chang, W. Song, Y. Hu, G. Shao, E. Sandraz, G. Zhang, L. Li, J. Wang, Magnetically Propelled fish-like nanoswimmers, Small 12 (2016) 6098–6105, doi:10.1002/smll.201601846.
[51] A.A. Solovev, S. Sanchez, M. Pumera, Y.F. Mei, O.C. Schmidt, Magnetic control of tubular catalytic microbots for the transport, assembly, and delivery of micro-objects, Adv. Funct. Mater. 20 (2010) 2430–2435, doi:10.1002/adfm.200902376.
[52] S. Palagi, P. Fischer, Bioinspired microrobots, Nat. Rev. Mater. 3 (2018) 113–124, doi:10.1038/s41578-018-0016-9.
[53] B. Jang, E. Gutman, N. Stucki, B.F. Seitz, P.D. Wendel-García, T. Newton, J. Pokki, O. Ergeneman, S. Pané, Y. Or, B.J. Nelson, Undulatory locomotion of magnetic multilink nanoswimmers, Nano Lett 15 (2015) 4829–4833, doi:10.1021/acs.nanolett.5b01981.
[54] J. Li, S. Sattayasamitsathit, R. Dong, W. Gao, R. Tam, X. Feng, S. Ai, J. Wang, Template electrosynthesis of tailored-made helical nanoswimmers, Nanoscale 6 (2014) 9415–9420, doi:10.1039/c3nr04760a.
[55] C. Peters, O. Ergeneman, P.D.W. García, M. Müller, S. Pané, B.J. Nelson, C. Hierold, Superparamagnetic twist-type actuators with shape-independent magnetic properties and surface functionalization for advanced biomedical applications, Adv. Funct. Mater. 24 (2014) 5269–5276, doi:10.1002/adfm.201400596.
[56] S. Kim, S. Lee, J. Lee, B.J. Nelson, L. Zhang, H. Choi, Fabrication and manipulation of ciliary microrobots with non-reciprocal magnetic actuation, Sci. Rep. 6 (2016) 1–9, doi:10.1038/srep30713.
[57] C.W. Shields, K. Han, F. Ma, T. Miloh, G. Yossifon, O.D. Velev, Supercolloidal Spinners: Complex Active Particles for Electrically Powered and Switchable Rotation, Adv. Funct. Mater 28 (2018) 1–7, doi:10.1002/adfm.201803465.
[58] S.T. Chang, V.N. Paunov, D.N. Petsev, O.D. Velev, Remotely powered self-propelling particles and micropumps based on miniature diodes, Nat. Mater. 6 (2007) 235–240, doi:10.1038/nmat1843.
[59] M. Sentic, G. Loget, D. Manojlovic, A. Kuhn, N. Sojic, Light-emitting electrochemical “swimmers, Angew. Chemie - Int. Ed. 51 (2012) 11284–11288, doi:10.1002/anie.201206227.
[60] G. Loget, A. Kuhn, Electric field-induced chemical locomotion of conducting objects, Nat. Commun. 2 (2011), doi:10.1038/ncomms1550.
[61] J. Li, T. Li, T. Xu, M. Kiristi, W. Liu, Z. Wu, J. Wang, Magneto-acoustic hybrid nanomotor, Nano Lett 15 (2015) 4814–4821, doi:10.1021/acs.nanolett.5b01945.
[62] D. Kagan, M.J. Benchimol, J.C. Claussen, E. Chuluun-Erdene, S. Esener, J. Wang, Acoustic droplet vaporization and propulsion of perfluorocarbon-loaded microbullets for targeted tissue penetration and deformation, Angew. Chemie - Int. Ed. 51 (2012) 7519–7522, doi:10.1002/anie.201201902.
[63] Q. Zhang, R. Dong, Y. Wu, W. Gao, Z. He, B. Ren, Light-Driven Au-WO3@C janus micromotors for rapid photodegradation of dye pollutants, ACS Appl. Mater. Interfaces. 9 (2017) 4674–4683, doi:10.1021/acsami.6b12081.
[64] X. Wang, L. Baraban, A. Nguyen, J. Ge, V.R. Misko, J. Tempere, F. Nori, P. Formanek, T. Huang, G. Cuniberti, J. Fassbender, D. Makarov, High-motility visible light-driven Ag/AgCl janus micromotors, Small 14 (2018) 1–11, doi:10.1002/smll.201803613.
[65] Y. Hong, M. Diaz, U.M. Córdova-Fteueroa, A. Sen, Light-driven titanium-dioxide-based reversible microfireworks and micromotor/micropump systems, Adv. Funct. Mater. 20 (2010) 1568–1576, doi:10.1002/adfm.201000063.
[66] S. Giudicatti, S.M. Marz, L. Soler, A. Madani, M.R. Jorgensen, S. Sanchez, O.G. Schmidt, Photoactive rolled-up TiO2 microtubes: Fabrication, characterization and applications, J. Mater. Chem. C. 2 (2014) 5892–5901, doi:10.1039/c4tc00796d.
[67] D. Zhou, Y.C. Li, P. Xu, N.S. McCool, L. Li, W. Wang, T.E. Mallouk, Visible-light controlled catalytic Cu2O-Au micromotors, Nanoscale 9 (2017) 75–78, doi:10.1039/c6nr08088j.
[68] C. Chen, S. Tang, H. Teymourian, E. Karshalev, F. Zhang, J. Li, F. Mou, Y. Liang, J. Guan, J. Wang, Chemical/light-powered hybrid micromotors with “On-the-Fly” optical brakes, Angew. Chemie - Int. Ed. 57 (2018) 8110–8114, doi:10.1002/anie.201803457.
[69] W. Gao, K.M. Manesh, J. Hua, S. Sattayasamitsathit, J. Wang, Hybrid nanomotor: a catalytically/magnetically powered adaptive nanowire swimmer, Small 7 (2011) 2047–2051, doi:10.1002/smll.201100213.
[70] L. Ren, D. Zhou, Z. Mao, P. Xu, T.J. Huang, T.E. Mallouk, Rheotaxis of bimetallic micromotors driven by chemical-acoustic hybrid power, ACS Nano 11 (2017) 10591–10598, doi:10.1021/acsnano.7b06107.

[71] S. Tang, F. Zhang, J. Zhao, W. Talaat, F. Soto, E. Karshalev, C. Chen, Z. Hu, X. Lu, J. Li, Z. Lin, H. Dong, X. Zhang, A. Nourhani, J. Wang, Structure-dependent optical modulation of propulsion and collective behavior of acoustic/light-driven hybrid microbowls, Adv. Funct. Mater. 29 (2019) 1–7, doi:10.1002/adfm.201809003.

[72] K. Yuan, V. De La Asunción-Nadal, B. Jurado-Sánchez, A. Escarpa, 2D nanomaterials wrapped janus micromotors with built-in multiengines for bubble, magnetic, and light driven propulsion, Chem. Mater. 32 (2020) 1983–1992, doi:10.1021/acs.chemmater.9b04873.

[73] S. Sanchez, A.A. Solovev, Y. Mei, O.G. Schmidt, Dynamics of biocatalytic microengines mediated by variable friction control, J. Am. Chem. Soc. 132 (2010) 13144–13145, doi:10.1021/ja104362r.

[74] N. Mano, A. Heller, Bioelectrochemical propulsion, J. Am. Chem. Soc. 127 (2005) 11574–11575, doi:10.1021/ja053937e.

[75] D. Pantarotto, W.R. Browne, B.L. Feringa, Autonomous propulsion of carbon nanotubes powered by a multienzyme ensemble, Chem. Commun. (2008) 1533–1535, doi:10.1039/b715310d.

[76] W. Gao, K.M. Manesh, J. Hua, S. Sattayasamitsathit, J. Wang, Hybrid nanomotor: A catalytically/magnetically powered adaptive nanowire swimmer, Small 7 (2011) 2047–2051, doi:10.1002/smll.201100213.

[77] D. Walker, B.T. Käsdorf, H.H. Jeong, O. Lieleg, P. Fischer, Biomolecules: enzymatically active biomimetic micropropellers for the penetration of mucin gels, Sci. Adv. 1 (2015) 33–35, doi:10.1126/sciadv.1500501.

[78] U. Choudhury, L. Soler, J.G. Gibbs, S. Sanchez, P. Fischer, Surface roughness-induced speed increase for active Janus micromotors, Chem. Commun. 51 (2015) 8660–8663, doi:10.1039/c5cc01607j.

[79] J. García-Torres, C. Calero, F. Sagués, I. Pagonabarraga, P. Tierno, Magnetically tunable bidirectional locomotion of a self-assembled nanorod-sphere propeller, Nat. Commun. 9 (2018) 1–7, doi:10.1038/s41467-018-04115-w.

[80] I.S.M. Khalil, H.C. Dijkslag, L. Abelmann, S. Misra, MagnetoSperm: a microrobot that navigates using weak magnetic fields, Appl. Phys. Lett. 104 (2014), doi:10.1063/1.4880035.

[81] W. Wang, Z. Wu, X. Lin, T. Si, Q. He, Gold-nanoshell-functionalized polymer nanoswimmer for photomechanical poration of single-cell membrane, J. Am. Chem. Soc. 141 (2019) 6601–6608, doi:10.1021/jacs.8b13882.

[82] Z. Wu, L. Li, Y. Yang, P. Hu, Y. Li, S.Y. Yang, L.V. Wang, W. Gao, A microrobotic system guided by photoacoustic computed tomography for targeted navigation in intestines in vivo, Sci. Robot. (2019) 4, doi:10.1126/scirobotics.aax0613.

[83] Z. Wu, J. Troll, H.H. Jeong, Q. Wei, M. Stang, F. Ziemssen, Z. Wang, M. Dong, S. Schnichels, T. Qiu, P. Fischer, A swarm of slippery micropropellers penetrates the vitreous body of the eye, Sci. Adv. 4 (2018) 1–10, doi:10.1126/sciadv.aat4388.

[84] J.G. Gibbs, N.A. Fragnito, Y. Zhao, Asymmetric Pt/Au coated catalytic micromotors fabricated by dynamic shadowing growth, Appl. Phys. Lett. 97 (2010) 3–6, doi:10.1063/1.3529448.

[85] P. Cabanach, A. Pena-Francesch, D. Sheehan, U. Bozuyuk, O. Yasa, S. Borros, M. Sitti, Zwitterionic 3D-printed non-immunogenic stealth microrobots, Adv. Mater. 32 (2020) 1–11, doi:10.1002/adma.202003013.

[86] M. Hoop, Y. Shen, X.Z. Chen, F. Mushtaq, L.M. Iuliano, M.S. Sakar, A. Petruska, M.J. Loessner, B.J. Nelson, S. Pané, Magnetically driven silver-coated nanocoils for efficient bacterial contact killing, Adv. Funct. Mater. 26 (2016) 1063–1069, doi:10.1002/adfm.201504463.

[87] J.G.S. Moo, C.C. Mayorga-Martinez, H. Wang, B. Khezri, W.Z. Teo, M. Pumera, Nano/microrobots meet electrochemistry, Adv. Funct. Mater. (2017) 27, doi:10.1002/adfm.201604759.

[88] H. Wang, M. Pumera, Fabrication of micro/nanoscale motors, Chem. Rev. 115 (2015) 8704–8735, doi:10.1021/acs.chemrev.5b00047.

[89] J. Li, I. Rozen, J. Wang, Rocket science at the nanoscale, ACS Nano 10 (2016) 5619–5634, doi:10.1021/acsnano.6b02518.

[90] J.P. Abid, M. Frigoli, R. Pansu, J. Szeftel, J. Zyss, C. Larpent, S. Brasselet, Light-driven directed motion of azobenzene-coated polymer nanoparticles in an aqueous medium, Langmuir 27 (2011) 7967–7971, doi:10.1021/la200682p.

[91] J. Berná, D.A. Leigh, M. Lubomska, S.M. Mendoza, E.M. Pérez, P. Rudolf, G. Teobaldi, F. Zerbetto, Macroscopic transport by synthetic molecular machines, Nat. Mater. 4 (2005) 704–710, doi:10.1038/nmat1455.

[92] M.E. Alea-Reyes, M. Rodrigues, A. Serrà, M. Mora, M.L. Sagristá, A. González, S. Durán, M. Duch, J.A. Plaza, E. Vallés, D.A. Russell, L. Pérez-García, Nanostructured materials for photodynamic therapy: synthesis, characterization and in vitro activity, RSC Adv 7 (2017) 16963–16976, doi:10.1039/c7ra01569k.

[93] A. Kumar, G. Sharma, M. Naushad, S. Thakur, SPION/β-cyclodextrin core-shell nanostructures for oil spill remediation and organic pollutant removal from waste water, Chem. Eng. J. 280 (2015) 175–187, doi:10.1016/j.cej.2015.05.126.

[94] A. Kumar, C. Guo, G. Sharma, D. Pathania, M. Naushad, S. Kalia, P. Dhiman, Magnetically recoverable ZrO2/Fe3O4/chitosan nanomaterials for enhanced sunlight driven photoreduction of carcinogenic Cr(VI) and dechlorination & mineralization of 4-chlorophenol from simulated waste water, RSC Adv 6 (2016) 13251–13263, doi:10.1039/c5ra23372k.

[95] L. Restrepo-Pérez, L. Soler, C. Martínez-Cisneros, S. Sánchez, O.G. Schmidt, Biofunctionalized self-propelled micromotors as an alternative on-chip concentrating system, Lab Chip 14 (2014) 2914–2917, doi:10.1039/c4lc00439f.

[96] A. Serrà, E. Vallés, J. García-Torres, Electrochemically synthesized nanostructures for the manipulation of cells: Biohybrid micromotors, Electrochem. Commun. 85 (2017) 27–31, doi:10.1016/j.elecom.2017.11.002.

[97] A. Serrà, G. Vázquez-Mariño, J. García-Torres, M. Bosch, E. Vallés, Magnetic actuation of multifunctional nanorobotic platforms to induce cancer cell death, Adv. Biosyst. 1700220 (2018) 1700220, doi:10.1002/adbi.201700220.

[98] H. Chen, D. Sulejmanovic, T. Moore, D.C. Colvin, B. Qi, O.T. Mefford, J.C. Gore, F. Alexis, S.J. Hwu, J.N. Anker, Iron-loaded magnetic nanocapsules for pH-triggered drug release and MRI imaging, Chem. Mater. 26 (2014) 2105–2112, doi:10.1021/cm404168a.

[99] E.M. Purcell, Life at low Reynolds number, Am. J. Phys. 45 (1977) 3–11, doi:10.1119/1.10903.

[100] M. Guix, C.C. Mayorga-Martinez, A. Merkoçi, Nano/Micromotors in (Bio)chemical science applications, Chem. Rev. 114 (2014) 6285–6322, doi:10.1021/cr400273r.

[101] U.K. Demirok, R. Laocharoensuk, K.M. Manesh, J. Wang, Ultrafast catalytic alloy nanomotors, Angew. Chemie - Int. Ed. 47 (2008) 9349–9351, doi:10.1002/anie.200803841.

[102] R. Laocharoensuk, J. Burdick, J. Wang, Carbon-nanotube-induced acceleration of catalytic nanomotors, ACS Nano 2 (2008) 1069–1075, doi:10.1021/nn800154g.

[103] J.R. Baylis, J.H. Yeon, M.H. Thomson, A. Kazerooni, X. Wang, A.E.S. John, E.B. Lim, D. Chien, A. Lee, J.Q. Zhang, J.M. Piret, L.S. Machan, T.F. Burke, N.J. White, C.J. Kastrup, Self-propelled particles that transport cargo through flowing blood and halt hemorrhage, Sci. Adv. 1 (2015) 1–9, doi:10.1126/sciadv.1500379.

[104] X. Ma, A. Jannasch, U.R. Albrecht, K. Hahn, A. Miguel-López, E. Schäffer, S. Sánchez, Enzyme-powered hollow mesoporous janus nanomotors, Nano Lett 15 (2015) 7043–7050, doi:10.1021/acs.nanolett.5b03100.

[105] Y. Ye, J. Luan, M. Wang, Y. Chen, D.A. Wilson, F. Peng, Y. Tu, Fabrication of self-propelled micro- and nanomotors based on janus structures, Chem. - A Eur. J. 25 (2019) 8663–8680, doi:10.1002/chem.201900840.

[106] M. Safdar, S.U. Khan, J. Jänis, Progress toward Catalytic Micro- and Nanomotors for Biomedical and Environmental Applications, Adv. Mater. 30 (2018) 1–27, doi:10.1002/adma.201703660.

[107] Z. Yang, L. Zhang, Magnetic actuation systems for miniature robots: a review, Adv. Intell. Syst. 2000082 (2020) 2000082, doi:10.1002/aisy.202000082.

[108] J. Li, S. Sattayasamitsathit, R. Dong, W. Gao, R. Tam, X. Feng, S. Ai, J. Wang, Template electrosynthesis of tailored-made helical nanoswimmers, Nanoscale 6 (2014) 9415–9420, doi:10.1039/c3nr04760a.

[109] D.Y. Nam, A.Y. Samardak, Y.S. Jeon, S.H. Kim, A.V. Davydenko, A.V. Ognev, A.S. Samardak, Y.K. Kim, Magnetization reversal of ferromagnetic nanosprings affected by helical shape, Nanoscale 10 (2018) 20405–20413, doi:10.1039/c8nr05655b.

[110] T. Li, J. Li, K.I. Morozov, Z. Wu, T. Xu, I. Rozen, A.M. Leshansky, L. Li, J. Wang, Highly efficient freestyle magnetic nanoswimmer, Nano Lett 17 (2017) 5092–5098, doi:10.1021/acs.nanolett.7b02383.

[111] C. Calero, J. García-Torres, A. Ortiz-Ambriz, F. Sagués, I. Pagonabarraga, P. Tierno, Direct measurement of Lighthill's energetic efficiency of a minimal magnetic microswimmer, Nanoscale 11 (2019) 18723–18729, doi:10.1039/c9nr05825g.

[112] C. Calero, J. García-Torres, A. Ortiz-Ambriz, F. Sagués, I. Pagonabarraga, P. Tierno, Propulsion and energetics of a minimal magnetic microswimmer, Soft Matter 16 (2020) 6673–6682, doi:10.1039/d0sm00564a.

[113] L. Bouffier, A. Kuhn, Design of a wireless electrochemical valve, Nanoscale 5 (2013) 1305–1309, doi:10.1039/c2nr32875e.

[114] M. Kaynak, A. Ozcelik, A. Nourhani, P.E. Lammert, V.H. Crespi, T.J. Huang, Acoustic actuation of bioinspired microswimmers, Lab Chip 17 (2017) 395–400, doi:10.1039/c6lc01272h.

[115] S. Ahmed, D.T. Gentekos, C.A. Fink, T.E. Mallouk, Self-assembly of nanorod motors into geometrically regular multimers and their propulsion by ultrasound, ACS Nano 8 (2014) 11053–11060, doi:10.1021/nn5039614.

[116] S. Sabrina, M. Tasinkevych, S. Ahmed, A.M. Brooks, M. Olvera De La Cruz, T.E. Mallouk, K.J.M. Bishop, Shape-directed microspinners powered by ultrasound, ACS Nano 12 (2018) 2939–2947, doi:10.1021/acsnano.8b00525.

[117] H.R. Jiang, N. Yoshinaga, M. Sano, Active motion of a Janus particle by self-thermophoresis in a defocused laser beam, Phys. Rev. Lett. 105 (2010) 1–4, doi:10.1103/PhysRevLett.105.268302.

[118] Y. Ji, X. Lin, H. Zhang, Y. Wu, J. Li, Q. He, Thermoresponsive polymer brush modulation on the direction of motion of phoretically driven janus micromotors, Angew. Chemie - Int. Ed. 58 (2019) 4184–4188, doi:10.1002/anie.201812860.

[119] Q. Cao, Q. Fan, Q. Chen, C. Liu, X. Han, L. Li, Recent advances in manipulation of micro- and nano-objects with magnetic fields at small scales, Mater. Horizons. 7 (2020) 638–666, doi:10.1039/c9mh00714h.

[120] X.Z. Chen, B. Jang, D. Ahmed, C. Hu, C. De Marco, M. Hoop, F. Mushtaq, B.J. Nelson, S. Pané, Small-scale machines driven by external power sources, Adv. Mater. 30 (2018) 1–22, doi:10.1002/adma.201705061.

[121] L. Xu, F. Mou, H. Gong, M. Luo, J. Guan, Light-driven micro/nanomotors: from fundamentals to applications, Chem. Soc. Rev. 46 (2017) 6905–6926, doi:10.1039/c7cs00516d.

[122] T. Xu, W. Gao, L.P. Xu, X. Zhang, S. Wang, Fuel-free synthetic micro-/nanomachines, Adv. Mater. (2017) 29, doi:10.1002/adma.201603250.

[123] Y. Tu, F. Peng, D.A. Wilson, Motion manipulation of micro- and nanomotors, Adv. Mater. 29 (2017) 1–20, doi:10.1002/adma.201701970.

[124] I.J. Alja Zottel, Alja videtic paska, nanotechnology meets oncology : nanomaterials, Materials (Basel) 12 (2019) 1–28.

[125] S. Li, Q. Jiang, S. Liu, Y. Zhang, Y. Tian, C. Song, J. Wang, Y. Zou, G.J. Anderson, J.Y. Han, Y. Chang, Y. Liu, C. Zhang, L. Chen, G. Zhou, G. Nie, H. Yan, B. Ding, Y. Zhao, A DNA nanorobot functions as a cancer therapeutic in response to a molecular trigger in vivo, Nat. Biotechnol. 36 (2018) 258–264, doi:10.1038/nbt.4071.

[126] K.R. Sharma, Nanorobot drug delivery system for curcumin for enhanced bioavailability during treatment of Alzheimer's disease, J. Encapsulation Adsorpt. Sci. 03 (2013) 24–34, doi:10.4236/jeas.2013.31004.
[127] N.P.S. Daniel E Shumer, Natalie J Nokoff, 乳鼠心肌提取 HHS Public Access, Physiol. Behav. 176 (2017) 139–148, doi:10.1016/j.physbeh.2017.03.040.
[128] N.J. Shetty, P. Swati, K. David, Nanorobots: future in dentistry, Saudi Dent. J. 25 (2013) 49–52, doi:10.1016/j.sdentj.2012.12.002.
[129] B. Jurado-Sánchez, J. Wang, Micromotors for environmental applications: a review, Environ. Sci. Nano. 5 (2018) 1530–1544, doi:10.1039/c8en00299a.
[130] L. Soler, S. Sánchez, Catalytic nanomotors for environmental monitoring and water remediation, Nanoscale 6 (2014) 7175–7182, doi:10.1039/c4nr01321b.
[131] L. Soler, V. Magdanz, V.M. Fomin, S. Sanchez, O.G. Schmidt, Self-propelled micromotors for cleaning polluted water, ACS Nano 7 (2013) 9611–9620, doi:10.1021/nn405075d.
[132] W. Wang, S. Li, L. Mair, S. Ahmed, T.J. Huang, T.E. Mallouk, Acoustic propulsion of nanorod motors inside living cells, Angew. Chemie. 126 (2014) 3265–3268, doi:10.1002/ange.201309629.
[133] W. Xi, A.A. Solovev, A.N. Ananth, D.H. Gracias, S. Sanchez, O.G. Schmidt, Rolled-up magnetic microdrillers: towards remotely controlled minimally invasive surgery, Nanoscale 5 (2013) 1294–1297, doi:10.1039/c2nr32798h.
[134] B.E.F. De Ávila, P. Angsantikul, J. Li, M. Angel Lopez-Ramirez, D.E. Ramírez-Herrera, S. Thamphiwatana, C. Chen, J. Delezuk, R. Samakapiruk, V. Ramez, L. Zhang, J. Wang, Micromotor-enabled active drug delivery for in vivo treatment of stomach infection, Nat. Commun. 8 (2017) 1–8, doi:10.1038/s41467-017-00309-w.
[135] Y. Tu, F. Peng, X. Sui, Y. Men, P.B. White, J.C.M. Van Hest, D.A. Wilson, Self-propelled supramolecular nanomotors with temperature-responsive speed regulation, Nat. Chem. 9 (2017) 480–486, doi:10.1038/nchem.2674.
[136] Z. Wu, Y. Chen, D. Mukasa, O.S. Pak, W. Gao, Medical micro/nanorobots in complex media, Chem. Soc. Rev. (2020), doi:10.1039/D0CS00309C.
[137] A. Serrà, E. Vallés, Advanced electrochemical synthesis of multicomponent metallic nanorods and nanowires: Fundamentals and applications, Appl. Mater. Today. 12 (2018) 207–234, doi:10.1016/j.apmt.2018.05.006.
[138] A.J. Yin, J. Li, W. Jian, A.J. Bennett, J.M. Xu, Fabrication of highly ordered metallic nanowire arrays by electrodeposition, Appl. Phys. Lett. 79 (2001) 1039–1041, doi:10.1063/1.1389765.
[139] Y. Sun, C. Liu, D.C. Grauer, J. Yano, J.R. Long, P. Yang, C.J. Chang, Electrodeposited cobalt-sulfide catalyst for electrochemical and photoelectrochemical hydrogen generation from water, J. Am. Chem. Soc. 135 (2013) 17699–17702, doi:10.1021/ja4094764.
[140] J. Wang, Template electrodeposition of catalytic nanomotors, Faraday Discuss 164 (2013) 9–18, doi:10.1039/c3fd00105a.
[141] B. Alshammary, F.C. Walsh, P. Herrasti, C. Ponce de Leon, Electrodeposited conductive polymers for controlled drug release: polypyrrole, J. Solid State Electrochem. 20 (2016) 839–859, doi:10.1007/s10008-015-2982-9.
[142] L. Besra, M. Liu, A review on fundamentals and applications of electrophoretic deposition (EPD), Prog. Mater. Sci. 52 (2007) 1–61, doi:10.1016/j.pmatsci.2006.07.001.
[143] G. Zhao, M. Pumera, Concentric bimetallic microjets by electrodeposition, RSC Adv 3 (2013) 3963–3966, doi:10.1039/c3ra23128c.
[144] A. Serrà, Y. Zhang, B. Sepúlveda, E. Gómez, J. Nogués, J. Michler, L. Philippe, Highly active ZnO-based biomimetic fern-like microleaves for photocatalytic water decontamination using sunlight, Appl. Catal. B Environ. 248 (2019) 129–146, doi:10.1016/j.apcatb.2019.02.017.
[145] A. Serrà, E. Gómez, L. Philippe, Bioinspired ZnO-based solar photocatalysts for the efficient decontamination of persistent organic pollutants and hexavalent chromium in wastewater, Catalysts 9 (2019) 1–16, doi:10.3390/catal9120974.
[146] A. Serrà, E. Vallés, Microemulsion-based one-step electrochemical fabrication of mesoporous catalysts, Catalysts 8 (2018) 1–22, doi:10.3390/catal8090395.
[147] S. Sattayasamitsathit, H. Kou, W. Gao, W. Thavarajah, K. Kaufmann, L. Zhang, J. Wang, Fully loaded micromotors for combinatorial delivery and autonomous release of cargoes, Small 10 (2014) 2830–2833, doi:10.1002/smll.201303646.
[148] P. Schürch, R. Ramachandramoorthy, L. Pethö, J. Michler, L. Philippe, Additive manufacturing by template-assisted 3D electrodeposition: nanocrystalline nickel microsprings and microspring arrays, Appl. Mater. Today. 18 (2020) 100472, doi:10.1016/j.apmt.2019.100472.
[149] P. Pip, C. Donnelly, M. Döbeli, C. Gunderson, L.J. Heyderman, L. Philippe, Electroless deposition of Ni–Fe alloys on scaffolds for 3D nanomagnetism, Small 2004099 (2020) 2004099, doi:10.1002/smll.202004099.
[150] A. Serrà, P. Pip, E. Gómez, L. Philippe, Efficient magnetic hybrid ZnO-based photocatalysts for visible-light-driven removal of toxic cyanobacteria blooms and cyanotoxins, Appl. Catal. B Environ. 268 (2020) 118745, doi:10.1016/j.apcatb.2020.118745.
[151] R.G. Raicheff, H.Z. Zahariev, Electrophoretic Deposition (1982) 33–39.
[152] S.J. Limmer, S. Seraji, M.J. Forbess, Y. Wu, T.P. Chou, C. Nguyen, G.Z. Cao, Electrophoretic growth of lead zirconate titanate nanorods, Adv. Mater. 13 (2001) 1269–1272, doi:10.1002/1521-4095(200108)13:16(1269::AID-ADMA1269)3.0.CO;2-S.
[153] A. Serrà, R. Artal, J. García-Amorós, B. Sepúlveda, E. Gómez, J. Nogués, L. Philippe, Hybrid Ni@ZnO@ZnS-microalgae for circular economy: a smart route to the efficient integration of solar photocatalytic water decontamination and bioethanol production, Adv. Sci. 7 (2020) 1–9, doi:10.1002/advs.201902447.
[154] A. Serrà, L. Philippe, Simple and scalable fabrication of hairy ZnO@ZnS core@shell Cu cables for continuous sunlight-driven photocatalytic water remediation, Chem. Eng. J. 401 (2020) 126164, doi:10.1016/j.cej.2020.126164.
[155] S. Guan, B.J. Nelson, Fabrication of hard magnetic microarrays by electroless codeposition for MEMS actuators, Sensors Actuators, A Phys 118 (2005) 307–312, doi:10.1016/j.sna.2004.08.020.
[156] R. Bernasconi, E. Carrara, M. Hoop, F. Mushtaq, X. Chen, B.J. Nelson, S. Pané, C. Credi, M. Levi, L. Magagnin, Magnetically navigable 3D printed multifunctional microdevices for environmental applications, Addit. Manuf. 28 (2019) 127–135, doi:10.1016/j.addma.2019.04.022.
[157] J. Izquierdo, L. Nagy, I. Bitter, R.M. Souto, G. Nagy, Potentiometric scanning electrochemical microscopy for the local characterization of the electrochemical behaviour of magnesium-based materials, Electrochim. Acta. 87 (2013) 283–293, doi:10.1016/j.electacta.2012.09.029.
[158] P.S. Nnamchi, C.S. Obayi, Electrochemical Characterization of Nanomaterials, Elsevier Ltd., 2018, doi:10.1016/B978-0-08-101973-3.00004-3.
[159] S.P. Kounaves, Voltammetric techniques, Inorg. Electrochem. (2007) 49–136, doi:10.1039/9781847551146-00049.
[160] Handbook of Nanoelectrochemistry : Electrochemical Synthesis Methods, Properties, and Characterization Techniques, 1st ed. 20, Springer International Publishing, Cham, n.d.
[161] D. Rojas, B. Jurado-Sánchez, A. Escarpa, Shoot and Sense" janus micromotors-based strategy for the simultaneous degradation and detection of persistent organic pollutants in food and biological samples, Anal. Chem. 88 (2016) 4153–4160, doi:10.1021/acs.analchem.6b00574.
[162] D. Martín-Yerga, Electrochemical detection and characterization of nanoparticles with printed devices, Biosensors 9 (2019), doi:10.3390/bios9020047.
[163] D. Zhou, Y.C. Li, P. Xu, N.S. McCool, L. Li, W. Wang, T.E. Mallouk, Visible-light controlled catalytic Cu2O-Au micromotors, Nanoscale 9 (2017) 75–78, doi:10.1039/c6nr08088j.
[164] J. Solla-Gullón, J.M. Feliu, State of the art in the electrochemical characterization of the surface structure of shape-controlled Pt, Au, and Pd nanoparticles, Curr. Opin. Electrochem. 22 (2020) 65–71, doi:10.1016/j.coelec.2020.04.010.
[165] M. Kiristi, V.V. Singh, B. Esteban-Fernández De Ávila, M. Uygun, F. Soto, D. Aktaş Uygun, J. Wang, Lysozyme-based antibacterial nanomotors, ACS Nano 9 (2015) 9252–9259, doi:10.1021/acsnano.5b04142.
[166] J. Orozco, L.A. Mercante, R. Pol, A. Merkoçi, Graphene-based Janus micromotors for the dynamic removal of pollutants, J. Mater. Chem. A. 4 (2016) 3371–3378, doi:10.1039/c5ta09850e.
[167] C. Zhou, H.P. Zhang, J. Tang, W. Wang, Photochemically powered AgCl janus micromotors as a model system to understand ionic self-diffusiophoresis, Langmuir 34 (2018) 3289–3295, doi:10.1021/acs.langmuir.7b04301.
[168] X. Wang, L. Baraban, V.R. Misko, F. Nori, T. Huang, G. Cuniberti, J. Fassbender, D. Makarov, Visible light actuated efficient exclusion between plasmonic Ag/AgCl micromotors and passive beads, Small (2018) 14, doi:10.1002/smll.201802537.
[169] V. Magdanz, G. Stoychev, L. Ionov, S. Sanchez, O.G. Schmidt, Stimuli-responsive microjets with reconfigurable shape, Angew. Chemie - Int. Ed. 53 (2014) 2673–2677, doi:10.1002/anie.201308610.
[170] D. Vilela, J. Orozco, G. Cheng, S. Sattayasamitsathit, M. Galarnyk, C. Kan, J. Wang, A. Escarpa, Multiplexed immunoassay based on micromotors and microscale tags, Lab Chip 14 (2014) 3505–3509, doi:10.1039/c4lc00596a.
[171] H. Ye, J. Kang, G. Ma, H. Sun, S. Wang, High-speed graphene@Ag-MnO2 micromotors at low peroxide levels, J. Colloid Interface Sci. 528 (2018) 271–280, doi:10.1016/j.jcis.2018.05.088.
[172] H. Wang, G. Zhao, M. Pumera, Blood electrolytes exhibit a strong influence on the mobility of artificial catalytic microengines, Phys. Chem. Chem. Phys. 15 (2013) 17277–17280, doi:10.1039/c3cp52726c.
[173] H. Wang, G. Zhao, M. Pumera, Blood proteins strongly reduce the mobility of artificial self-propelled micromotors, Chem. - A Eur. J. 19 (2013) 16756–16759, doi:10.1002/chem.201301906.
[174] E.L. Khim Chng, G. Zhao, M. Pumera, Towards biocompatible nano/microscale machines: Self-propelled catalytic nanomotors not exhibiting acute toxicity, Nanoscale 6 (2014) 2119–2124, doi:10.1039/c3nr04997c.
[175] S. Sanchez, L. Soler, J. Katuri, Chemically powered micro- and nanomotors, Angew. Chemie - Int. Ed. 54 (2015) 1414–1444, doi:10.1002/anie.201406096.
[176] Y. Yoshizumi, H. Suzuki, Self-propelled metal-polymer hybrid micromachines with bending and rotational motions, ACS Appl. Mater. Interfaces. 9 (2017) 21355–21361, doi:10.1021/acsami.7b03656.
[177] G. Zhao, A. Ambrosi, M. Pumera, Clean room-free rapid fabrication of roll-up self-powered catalytic microengines, J. Mater. Chem. A. 2 (2014) 1219–1223, doi:10.1039/c3ta14318j.
[178] J. Orozco, B. Jurado-Sánchez, G. Wagner, W. Gao, R. Vazquez-Duhalt, S. Sattayasamitsathit, M. Galarnyk, A. Cortés, D. Saintillan, J. Wang, Bubble-propelled micromotors for enhanced transport of passive tracers, Langmuir 30 (2014) 5082–5087, doi:10.1021/la500819r.
[179] J. Orozco, G. Pan, S. Sattayasamitsathit, M. Galarnyk, J. Wang, Micromotors to capture and destroy anthrax simulant spores, Analyst 140 (2015) 1421–1427, doi:10.1039/c4an02169j.
[180] Y. Li, J. Wu, Y. Xie, H. Ju, An efficient polymeric micromotor doped with Pt nanoparticle@carbon nanotubes for complex bio-media, Chem. Commun. 51 (2015) 6325–6328, doi:10.1039/c5cc00546a.
[181] V.V. Singh, A. Martin, K. Kaufmann, S.D.S. De Oliveira, J. Wang, Zirconia/graphene oxide hybrid micromotors for selective capture of nerve agents, Chem. Mater. 27 (2015) 8162–8169, doi:10.1021/acs.chemmater.5b03960.

[182] M. Safdar, O.M. Wani, J. Jänis, Manganese oxide-based chemically powered micromotors, ACS Appl. Mater. Interfaces. 7 (2015) 25580–25585, doi:10.1021/acsami.5b08789.
[183] R. Maria-Hormigos, B. Jurado-Sánchez, A. Escarpa, Labs-on-a-chip meet self-propelled micromotors, Lab Chip 16 (2016) 2397–2407, doi:10.1039/c6lc00467a.
[184] V.D. La Asunción-Nadal, B. Jurado-Sánchez, L. Vázquez, A. Escarpa, Near infrared-light responsive WS2 microengines with high-performance electro-And photo-catalytic activities, Chem. Sci. 11 (2020) 132–140, doi:10.1039/c9sc03156a.
[185] H. Wang, J.G.S. Moo, M. Pumera, From nanomotors to micromotors: the influence of the size of an autonomous bubble-propelled device upon its motion, ACS Nano 10 (2016) 5041–5050, doi:10.1021/acsnano.5b07771.
[186] V.V. Singh, K. Kaufmann, B.E.F. de Ávila, E. Karshalev, J. Wang, Molybdenum disulfide-based tubular microengines: toward biomedical applications, Adv. Funct. Mater. 26 (2016) 6270–6278, doi:10.1002/adfm.201602005.
[187] Y. Wang, C.C. Mayorga-Martinez, J.G.S. Moo, M. Pumera, Structure-function dependence on template-based micromotors, ACS Appl. Energy Mater. 1 (2018) 3443–3448, doi:10.1021/acsaem.8b00605.
[188] S.M. Beladi-Mousavi, B. Khezri, L. Krejčová, Z. Heger, Z. Sofer, A.C. Fisher, M. Pumera, Recoverable bismuth-based microrobots: capture, transport, and on-demand release of heavy metals and an anticancer drug in confined spaces, ACS Appl. Mater. Interfaces. 11 (2019) 13359–13369, doi:10.1021/acsami.8b19408.
[189] M. Luo, Y. Jiang, J. Su, Z. Deng, F. Mou, L. Xu, J. Guan, Surface charge-reversible tubular micromotors for extraction of nucleic acids in microsystems, Chem. - An Asian J. 14 (2019) 2503–2511, doi:10.1002/asia.201900427.
[190] L. Liu, S.H. Yoo, S.A. Lee, S. Park, Wet-chemical synthesis of palladium nanosprings, Nano Lett 11 (2011) 3979–3982, doi:10.1021/nl202332x.
[191] M.A. Zeeshan, R. Grisch, E. Pellicer, K.M. Sivaraman, K.E. Peyer, J. Sort, B. Özkale, M.S. Sakar, B.J. Nelson, S. Pané, Hybrid helical magnetic microrobots obtained by 3D template-assisted electrodeposition, Small 10 (2014) 1284–1288, doi:10.1002/smll.201302856.
[192] G. Chatzipirpiridis, C. de Marco, E. Pellicer, O. Ergeneman, J. Sort, B.J. Nelson, S. Pané, Template-assisted electroforming of fully semi-hard-magnetic helical microactuators, Adv. Eng. Mater. 20 (2018) 1–5, doi:10.1002/adem.201800179.
[193] S. Schuerle, S. Pané, E. Pellicer, J. Sort, M.D. Baró, B.J. Nelson, Helical and tubular lipid microstructures that are electroless-coated with conirep for wireless magnetic manipulation, Small 8 (2012) 1498–1502, doi:10.1002/smll.201101821.
[194] M. Guix, J. Orozco, M. Garcia, W. Gao, S. Sattayasamitsathit, A. Merkoči, A. Escarpa, J. Wang, Superhydrophobic alkanethiol-coated microsubmarines for effective removal of oil, ACS Nano 6 (2012) 4445–4451, doi:10.1021/nn301175b.
[195] H. Wang, B. Khezri, M. Pumera, Catalytic DNA-Functionalized Self-Propelled Micromachines for Environmental Remediation, Chem 1 (2016) 473–481, doi:10.1016/j.chempr.2016.08.009.
[196] D. Vilela, J. Parmar, Y. Zeng, Y. Zhao, S. Sánchez, Graphene-based microbots for toxic heavy metal removal and recovery from water, Nano Lett. 16 (2016) 2860–2866, doi:10.1021/acs.nanolett.6b00768.
[197] M. Uygun, V.V. Singh, K. Kaufmann, D.A. Uygun, S.D.S. De Oliveira, J. Wang, Micromotor-based biomimetic carbon dioxide sequestration: towards mobile microscrubbers, Angew. Chemie - Int. Ed. 54 (2015) 12900–12904, doi:10.1002/anie.201505155.
[198] J. Orozco, G. Cheng, D. Vilela, S. Sattayasamitsathit, R. Vazquez-Duhalt, G. Valdés-Ramírez, O.S. Pak, A. Escarpa, C. Kan, J. Wang, Micromotor-based high-yielding fast oxidative detoxification of chemical threats, Angew. Chemie - Int. Ed. 52 (2013) 13276–13279, doi:10.1002/anie.201308072.
[199] J. García-Torres, A. Serrà, P. Tierno, X. Alcobé, E. Vallés, Magnetic propulsion of recyclable catalytic nanocleaners for pollutant degradation, ACS Appl. Mater. Interfaces. 9 (2017) 23859–23868, doi:10.1021/acsami.7b07480.
[200] F. Mushtaq, M. Guerrero, M.S. Sakar, M. Hoop, A.M. Lindo, J. Sort, X. Chen, B.J. Nelson, E. Pellicer, S. Pané, Magnetically driven Bi2O3/BiOCl-based hybrid microrobots for photocatalytic water remediation, J. Mater. Chem. A. 3 (2015) 23670–23676, doi:10.1039/c5ta05825b.
[201] F. Mushtaq, A. Asani, M. Hoop, X.Z. Chen, D. Ahmed, B.J. Nelson, S. Pané, Highly efficient coaxial TiO2-PtPd tubular nanomachines for photocatalytic water purification with multiple locomotion strategies, Adv. Funct. Mater. 26 (2016) 6995–7002, doi:10.1002/adfm.201602315.
[202] D. Kagan, P. Calvo-Marzal, S. Balasubramanian, S. Sattayasamitsathit, K.M. Manesh, G.U. Flechsig, J. Wang, Chemical sensing based on catalytic nanomotors: Motion-based detection of trace silver, J. Am. Chem. Soc. 131 (2009) 12082–12083, doi:10.1021/ja905142q.
[203] J.G.S. Moo, H. Wang, G. Zhao, M. Pumera, Biomimetic artificial inorganic enzyme-free self-propelled microfish robot for selective detection of Pb2+ in water, Chem. - A Eur. J. 20 (2014) 4292–4296, doi:10.1002/chem.201304804.
[204] J. Orozco, V. García-Gradilla, M. D'Agostino, W. Gao, A. Cortés, J. Wang, Artificial enzyme-powered microfish for water-quality testing, ACS Nano 7 (2013) 818–824, doi:10.1021/nn305372n.
[205] V.V. Singh, K. Kaufmann, B. Esteban-Fernández De Ávila, M. Uygun, J. Wang, Nanomotors responsive to nerve-agent vapor plumes, Chem. Commun. 52 (2016) 3360–3363, doi:10.1039/c5cc10670b.
[206] B. Jurado-Sánchez, A. Escarpa, J. Wang, Lighting up micromotors with quantum dots for smart chemical sensing, Chem. Commun. 51 (2015) 14088–14091, doi:10.1039/c5cc04726a.
[207] B. Esteban-Fernández De Ávila, M.A. Lopez-Ramirez, D.F. Báez, A. Jodra, V.V. Singh, K. Kaufmann, J. Wang, Aptamer-modified graphene-based catalytic micromotors: off-on fluorescent detection of ricin, ACS Sensors 1 (2016) 217–221, doi:10.1021/acssensors.5b00300.
[208] Á. Molinero-Fernández, M. Moreno-Guzmán, M.Á. López, A. Escarpa, Biosensing strategy for simultaneous and accurate quantitative analysis of mycotoxins in food samples using unmodified graphene micromotors, Anal. Chem. 89 (2017) 10850–10857, doi:10.1021/acs.analchem.7b02440.
[209] Á. Molinero-Fernández, A. Jodra, M. Moreno-Guzmán, M.Á. López, A. Escarpa, Magnetic reduced graphene oxide/nickel/platinum nanoparticles micromotors for mycotoxin analysis, Chem. - A Eur. J. 24 (2018) 7172–7176, doi:10.1002/chem.201706095.